High frequency attenuation of elastic waves transmitted at an angle through a randomly-fluctuating horizontally-layered slab

M. Colvez, R. Cottereau

High frequency attenuation of elastic waves transmitted at an angle through a randomly-fluctuating horizontally-layered slab

M. Colvez[a], R. Cottereau[b]

[a] *Laboratoire de Mécanique Paris-Saclay, Université Paris-Saclay, CentraleSupélec, ENS Paris-Saclay, CNRS, Gif sur Yvette, France*
[b] *Aix-Marseille Univ, CNRS, Centrale Marseille, LMA UMR 7031, Marseille, France*

Abstract

This paper is concerned with the modeling of elastic waves travelling at small incidence angles through a randomly-fluctuating horizontally-layered slab, in regimes where the wavelength is small compared to the thickness of the slab. The wave propagation problem is reset in a frame following the coherent front, which propagates in a homogenized medium. This homogenized medium is anisotropic because of the layering, and the equations obtained account explicitly for the coupling of quasi-P and quasi-S waves. The resulting model is governed by a set of coupled stochastic ordinary differential equations that can be approximated numerically very efficiently, and yields in particular estimates of the transmission and reflections coefficients of the slab. The latter compare favorably to the coefficients obtained in a full scale numerical simulation of the (micro-scale) wave equation, for a fraction of the cost.

Keywords: Waves in random media, Waves in heterogeneous media, Dynamic homogenization, Localization, Elastic waves

2010 MSC: 00-01, 99-00

⋆This work was performed using HPC resources from the "Mésocentre" computing center of CentraleSupélec and École Normale Supérieure Paris-Saclay supported by CNRS and Région Île-de-France.

Email address: regis.cottereau@cnrs.fr (R. Cottereau)

1. Introduction

In many applications, for instance in seismic engineering [1], exploration geophysics [2] or non-destructive evaluation of composite media [3, 4], waves propagate large distances in rapidly-fluctuating media that are approximately horizontally-stratified. Computing accurately the wave patterns in these situations is very difficult, and the precise knowledge of the mechanical properties is in general not even available. In that case, modeling the mechanical properties as realizations of random fields provides an alternative approach, that yields homogenized results in terms of averages, such as average transmitted amplitudes. For instance, when the amplitude of the fluctuations is small and in the setting of the Rytov approximation [5], the O'Doherty-Anstey formula for normal waves [6] (and its generalization to oblique and elastic waves [2]) relate the transmission coefficient to the correlation of the material parameters, the frequency and the ratio of propagation distance to correlation length. The same problem is tackled in [7], choosing a different asymptotic ansatz (closer to Born than Rytov) and assuming a more precise asymptotic relation between the amplitude of the fluctuations of the material parameters, the correlation length, the wavelength and the propagation distance (see the discussion in [2, section 5.7]). Although more mathematically sound, the case of elastic materials with oblique waves was not treated with the latter approach [7].

The objective of this paper is therefore to derive an equation for the transmission coefficient of an oblique wave in a randomly-fluctuating horizontally-layered elastic medium. Both the cases of incident P-wave and incident S-wave will be treated, providing in each case a transmission coefficient towards P-waves and S-waves, while only the P→P and S→S coefficients were derived in [2]. Besides the one-dimensional character of the random medium, the main hypotheses are that the ratio of wavelength λ to propagation distance L and correlation length ℓ_c to propagation length are small ($\lambda/L \approx \ell_c/L \approx \epsilon \ll 1$) as well as the variance of the fluctuations ($\sigma^2 \approx \epsilon$), and that the angle of incidence of the incoming wave is small. Contrarily to the scalar case treated in [7], a closed formula will

not be obtained for the transmission coefficients, but the solution of the resulting 1D system of Stochastic Differential Equations (SDE) can be numerically approximated very efficiently.

The outline of this paper is the following: in the next section (Section 2), the elastodynamics equation is introduced and separated into two independent systems: one for the scalar SH wave, and one for the coupled P-SV waves. The SH case will be treated in Section 3, essentially summarizing the known approach and results of [7]. The main results of this paper will be derived in Section 4, that considers the coupled P-SV system. In that case it is necessary to assume that the angle of incidence is small enough that there is no degeneracy of the system (if the velocities of the quasi-P and quasi-S waves of the homogenized orthotropic equation become equal). Finally, in Section 5.4, a discretization of the resulting SDE is proposed and transmission coefficients are computed for a series of examples, and compared to full 3D simulations of the wave equation (using a Spectral Element Solver), as well as to the O-Doherty-Anstey formula [6, 2].

2. Elastodynamic wave equation for a random slab

In this section, we introduce the heterogeneous wave equation and separate it into two parts: a scalar SH wave, and a coupled P-SV wave system. Fourier transforms are considered in both the time and the horizontal direction in order to formulate the driving equations as ordinary differential equations in the vertical variable, whose parameters are random fields indexed on that same variable.

2.1. Geometry of the slab and full elastodynamics system

We consider a geometry (see Fig. 1) composed of a horizontal slab Ω, of finite thickness L, that is $\Omega = \{(\mathbf{x}, z), 0 < z < L\}$, where $\mathbf{x} = (x, y)$ denotes the horizontal components. This slab is sandwiched between two half-spaces $\Omega^- = \{(\mathbf{x}, z), z < 0\}$ and $\Omega^+ = \{(\mathbf{x}, z), L < z\}$. The equilibrium equation

states that, for any $t \geq 0$:

$$\nabla \cdot \sigma = \rho \frac{\partial \mathbf{v}}{\partial t}, \quad (\mathbf{x}, z) \in \Omega^- \cup \Omega \cup \Omega^+, \tag{1}$$

where $\sigma(\mathbf{x}, z, t)$ denotes the stress tensor, $\mathbf{v}(\mathbf{x}, z, t)$ the velocity vector, and the density ρ is assumed homogeneous.

Assuming small deformations and that the behavior of the slab is elastic, the constitutive relation in the slab is, for any $t \geq 0$:

$$\frac{\partial \sigma}{\partial t} = (K(z) - 2\mu(z)) (\nabla \cdot \mathbf{v}) \mathbf{I} + \mu(z) \left(\nabla \mathbf{v} + (\nabla \mathbf{v})^T \right), \quad (\mathbf{x}, z) \in \Omega, \tag{2}$$

where $\mathbf{I}$ denotes the identity tensor, and the superscrit ^{T} denotes transposition. Note that the P-wave $K(z)$ and shear $\mu(z)$ moduli only depend on the vertical variable z. We additionally introduce the compressional wave velocity $c_{\mathrm{P}}(z) = \sqrt{K(z)/\rho}$, shear wave velocity $c_{\mathrm{S}}(z) = \sqrt{\mu(z)/\rho}$ and their ratio $\alpha(z) = c_{\mathrm{S}}(z)/c_{\mathrm{P}}(z) < 1$. In order to simplify as much as possible the reading of the core of the text, and insist on the important concepts rather than technicalities, the P-wave modulus K is hereafter assumed homogeneous, and the P-wave velocity will be denoted $\overline{c_{\mathrm{P}}}$. In Appendix B, the case where both the bulk and shear moduli are heterogeneous is treated.

The shear modulus in the slab is modeled as a statistically stationary random process with a given probability law. More precisely, the shear modulus in the slab is modeled as

$$\frac{1}{\mu(z)} = \frac{1}{\overline{\mu}} (1 + \nu(z)), \quad 0 \leq z \leq L, \tag{3}$$

where $\nu(z)$ is the restriction to $[0, L]$ of a z-homogeneous Markov ergodic process, centered $\mathbb{E}[\nu(z)] = 0$, with given autocovariance $C_\nu(z) = \mathbb{E}[\nu(0)\nu(z)]$, variance $\sigma_\nu^2 = C_\nu(0)$, correlation length $\ell_c = \int_{\mathbb{R}} C_\nu(z) dz / \sigma_\nu^2$, and $\overline{\mu} = \mathbb{E}[1/\mu(z)]^{-1}$ is the harmonic average of $\mu(z)$.

The constitutive relation of the two half-spaces is given under Voigt notation ($\sigma = (\sigma_{xx}, \sigma_{yy}, \sigma_{zz}, \sigma_{yz}, \sigma_{xz}, \sigma_{xy})^T$ and $\epsilon = (\epsilon_{xx}, \epsilon_{yy}, \epsilon_{zz}, 2\epsilon_{yz}, 2\epsilon_{xz}, 2\epsilon_{xy})^T$), for

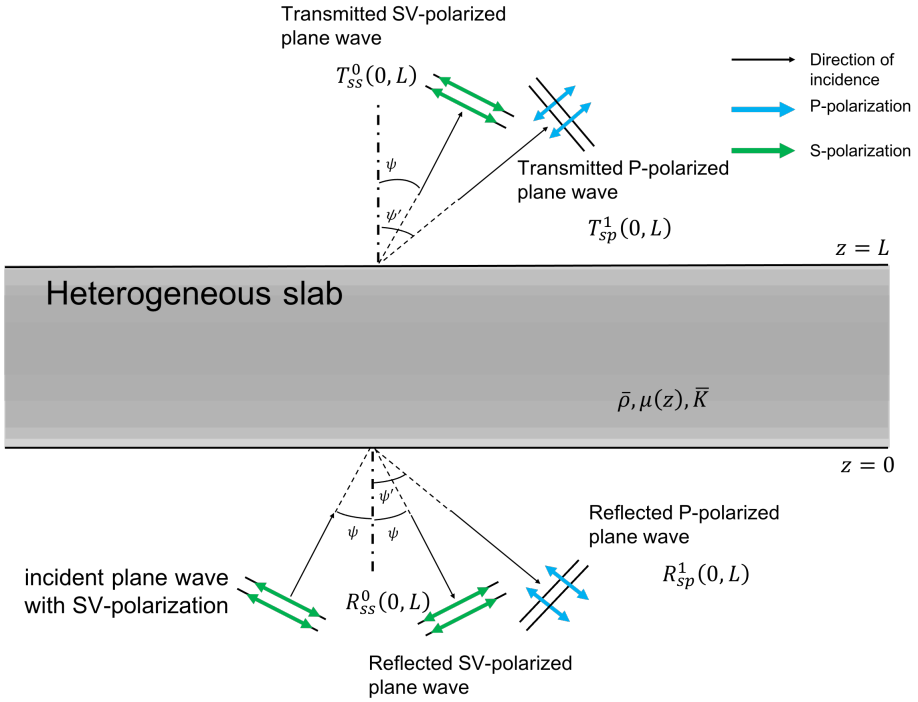

Figure 1: Representation of the wave propagation of an SV-polarized plane wave arriving with incidence angle ψ on a random slab. The reflected waves are located upstream and can be decomposed as a P-polarized wave associated to angle $\psi' \neq \psi$ and a S-polarized wave. The transmitted waves are located downstream the random slab and can be decomposed with the same polarization and the same angles as the reflected wave (the coefficients $\mathrm{T}_{\mathrm{SS}}^0$, $\mathrm{R}_{\mathrm{SS}}^0$, $\mathrm{T}_{\mathrm{SP}}^1$ and $\mathrm{R}_{\mathrm{SP}}^1$ are defined in Eq. (58) and 59).

$(\mathbf{x}, z) \in \Omega^- \cup \Omega^+$, by

$$\frac{\partial \sigma}{\partial t} = \rho \begin{bmatrix} \overline{c_{\mathrm{P}}}^2 & \overline{c_{\mathrm{P}}}^2 - 2\overline{c_{\mathrm{Sh}}}^2 & \overline{c_{\mathrm{P}}}^2 - 2\overline{c_{\mathrm{Sh}}}^2 & 0 & 0 & 0 \\ \overline{c_{\mathrm{P}}}^2 - 2\overline{c_{\mathrm{Sh}}}^2 & \overline{c_{\mathrm{P}}}^2 & \overline{c_{\mathrm{P}}}^2 - 2\overline{c_{\mathrm{Sh}}}^2 & 0 & 0 & 0 \\ \overline{c_{\mathrm{P}}}^2 - 2\overline{c_{\mathrm{Sh}}}^2 & \overline{c_{\mathrm{P}}}^2 - 2\overline{c_{\mathrm{Sh}}}^2 & \overline{c_{\mathrm{P}}}^2 & 0 & 0 & 0 \\ 0 & 0 & 0 & \overline{c_{\mathrm{S}}}^2 & 0 & 0 \\ 0 & 0 & 0 & 0 & \overline{c_{\mathrm{S}}}^2 & 0 \\ 0 & 0 & 0 & 0 & 0 & \overline{c_{\mathrm{Sh}}}^2 \end{bmatrix} \frac{\partial \epsilon}{\partial t} \tag{4}$$

where $\partial\epsilon/\partial t = (\nabla \mathbf{v} + (\nabla \mathbf{v})^T)/2$ and the coefficients are related to those of the

slab by

$$\overline{c_{\mathrm{S}}}^2 = \mathbb{E}\left[\frac{1}{c_{\mathrm{S}}^2(z)}\right]^{-1}, \quad \overline{c_{\mathrm{Sh}}}^2 = \mathbb{E}\left[c_{\mathrm{S}}^2(z)\right]. \tag{5}$$

The parameters of the half-spaces are thus those of a homogenized slab, which is orthotropic because of the layering of the slab (see [8] for details). This choice means that (in the asymptotic regime considered below), there is no average impedance mismatch between the half-spaces and the slab, and hence no reflection on average at the interfaces (see for instance [7, Chapter 4] for more details in the acoustic case). As with the homogeneous P-wave modulus, this hypothesis of matching half-spaces is not necessary but allows to simplify some technicalities (without removing any significantly interesting feature). Note that we will consider in this paper very weak contrast in the properties (small amplitude of the fluctuations of $\nu(z)$) so no propagating interface wave (such as Stoneley waves for instance) are expected to take place. More specifically we expect these effects to vanish in the limit of vanishing fluctuations that we will consider further down.

2.2. Systems of ordinary differential equations with random properties

As the properties and geometry of the problem of interest are invariant in the horizontal directions, we perform a Fourier transform in these directions. We are also interested in harmonic analysis so we perform an additional Fourier transform in time:

$$\begin{aligned}\hat{\mathbf{v}}\left(\kappa, z, \omega\right) &= \int_{\mathbb{R}^2}\int_{\mathbb{R}} e^{i\omega(t-\boldsymbol{\kappa}\cdot\mathbf{x})}\mathbf{v}(\mathbf{x}, z, t)\mathrm{d}t\mathrm{d}\mathbf{x} \\ \hat{\sigma}\left(\kappa, z, \omega\right) &= \int_{\mathbb{R}^2}\int_{\mathbb{R}} e^{i\omega(t-\boldsymbol{\kappa}\cdot\mathbf{x})}\sigma(\mathbf{x}, z, t)\mathrm{d}t\mathrm{d}\mathbf{x}\end{aligned} \tag{6}$$

We define the axes so that the wave vector is perpendicular to $\mathbf{e}_y$ (the axis orthogonal to the plane of the Fig. 1), so by definition $\boldsymbol{\kappa}\cdot\mathbf{e}_y = 0$, and the y-derivative of the velocity field and stresses vanishes. Note that the number $\kappa = \boldsymbol{\kappa}\cdot\mathbf{e}_x$ is not the classical wave number $\|\boldsymbol{\kappa}\|$, but rather the amplitude of the horizontal wave vector, with the incidence angle denoted ψ (and $\sin\psi = \kappa/\|\boldsymbol{\kappa}\|$, see Fig. 1). Note also that it is normalized by ω so it bears the units of a slowness.

These choices imply that Eq. (2) can be written into two uncoupled groups of equations. The first system describes the so-called SH wave:

$$\frac{d}{dz}\begin{bmatrix}\hat{v}_y\\ \hat{\sigma}_{yz}\end{bmatrix} = i\omega\begin{bmatrix}0 & (\rho c_{\mathrm{S}}^2)^{-1}\\ \rho(1-\kappa^2 c_{\mathrm{S}}^2) & 0\end{bmatrix}\begin{bmatrix}\hat{v}_y\\ \hat{\sigma}_{yz}\end{bmatrix}. \tag{7}$$

The second system describes the coupled behavior of the so-called P and SV waves:

$$\frac{d}{dz}\begin{bmatrix}\hat{v}_x\\ \hat{\sigma}_{xz}\\ \hat{v}_z\\ \hat{\sigma}_{zz}\end{bmatrix} = i\omega\begin{bmatrix}0 & (\rho c_{\mathrm{S}}^2)^{-1} & -\kappa & 0\\ \rho(1-4\kappa^2(1-\alpha^2)c_{\mathrm{S}}^2) & 0 & 0 & -\kappa(1-2\alpha^2)\\ -\kappa(1-2\alpha^2) & 0 & 0 & (\rho\overline{c_{\mathrm{P}}}^2)^{-1}\\ 0 & -\kappa & \rho & 0\end{bmatrix}\begin{bmatrix}\hat{v}_x\\ \hat{\sigma}_{xz}\\ \hat{v}_z\\ \hat{\sigma}_{zz}\end{bmatrix}. \tag{8}$$

Note that, in the case of vertically-incident waves, for which $\kappa = 0$, this second system decouples itself into two systems, one for the P waves, and one for the SV wave. In that case, the system for the SV wave is exactly the same as Eq. (7), and the system for the P wave is of the same form, but with $\overline{c_{\mathrm{P}}}$ instead of c_{S}.

2.3. Choice of asymptotic regime

We focus our attention on the so-called weak scattering regime [7, Chapter 5], where the wavelength λ, the correlation length ℓ_c, the propagation distance L and the variance σ_ν^2 verify

$$\frac{\ell_c}{\lambda} \sim 1, \quad \frac{L}{\lambda} \gg 1, \quad \sigma_\nu^2 \ll 1 \tag{9}$$

More precisely, we introduce a small quantity ϵ, and consider the following scalings:

$$\lambda \approx \epsilon^2 \quad \ell_c \approx \epsilon^2, \quad L \approx 1, \quad \sigma_\nu \approx \epsilon \tag{10}$$

With respect to Eq. (7) and (8), this means that in the regime of interest, the frequency is rescaled as ω/ϵ^2 and the random process is rescaled as $\epsilon\nu(z/\epsilon^2)$.

3. Transmission coefficient for a SH wave

In this section, we consider the system of Eq. (7), and show that, in the weak scattering regime introduced in Section 2.3, localization takes place in the

slab, prohibiting the transport of energy to the other side, provided it is thick enough. This localization takes place over a distance $L_{\mathrm{SH}}^{\mathrm{loc}}(\omega)$, depending on the frequency ω of the incident wave. Only the main steps are recalled and more details can be found in [7]. These steps can be broadly summarized as:

1. Projection of the wave equation on a modal basis (up-going and down-going modes)
2. Recentering of the modes to follow the coherent front
3. Transformation of the boundary value problem into a problem with initial conditions for the so-called propagator
4. Homogenized SDE (for small ϵ) for the propagator

Eventually, this sequence of steps and the resulting homogenized equation for the propagator yield the transmission coefficient. In this scalar case, in the limit of large thickness L, this transmission coefficient can be described by an explicit formula.

3.1. Projection on a modal basis

The first step consists in projecting Eq. (7) on a basis of eigenmodes of a well-chosen homogenized medium, which in this simple case follows the same equation, with homogeneous velocity $\overline{c_{\mathrm{S}}}$ (see Eq. (5)). These eigenmodes are gathered in matrix $\overline{\mathbf{M}}_{\mathrm{SH}}$:

$$\overline{\mathbf{M}}_{\mathrm{SH}} = \frac{1}{\sqrt{2}} \begin{bmatrix} \overline{\xi_{\mathrm{S}}}^{-1/2} & \overline{\xi_{\mathrm{S}}}^{-1/2} \\ \overline{\xi_{\mathrm{S}}}^{1/2} & -\overline{\xi_{\mathrm{S}}}^{1/2} \end{bmatrix}, \quad \overline{\mathbf{M}}_{\mathrm{SH}}^{-1} = \frac{1}{\sqrt{2}} \begin{bmatrix} \overline{\xi}_{\mathrm{S}}^{1/2} & \overline{\xi}_{\mathrm{S}}^{-1/2} \\ \overline{\xi}_{\mathrm{S}}^{1/2} & -\overline{\xi}_{\mathrm{S}}^{-1/2} \end{bmatrix}, \tag{11}$$

where $\overline{\xi_{\mathrm{S}}} = \rho \overline{c_{\mathrm{S}}}^2 / \overline{c_{\mathrm{S}\kappa}}$ and $\overline{c_{\mathrm{S}\kappa}}^2 = \overline{c_{\mathrm{S}}}^2 / (1 - \kappa^2 \overline{c_{\mathrm{S}}}^2)$. These modes correspond to eigenvalues $\lambda_{\mathrm{SH}} = \pm 1/\overline{c_{\mathrm{S}\kappa}}$. Eq. (7) can then be rewritten as

$$\frac{d}{dz} \begin{bmatrix} \hat{A}_{\mathrm{SH}} \\ \hat{B}_{\mathrm{SH}} \end{bmatrix} = \frac{i\omega}{\epsilon^2 \overline{c_{\mathrm{S}\kappa}}} \begin{bmatrix} \Delta_{\mu\kappa}^{(+)}\left(\frac{z}{\epsilon^2}\right) & \Delta_{\mu\kappa}^{(-)}\left(\frac{z}{\epsilon^2}\right) \\ -\Delta_{\mu\kappa}^{(-)}\left(\frac{z}{\epsilon^2}\right) & -\Delta_{\mu\kappa}^{(+)}\left(\frac{z}{\epsilon^2}\right) \end{bmatrix} \begin{bmatrix} \hat{A}_{\mathrm{SH}} \\ \hat{B}_{\mathrm{SH}} \end{bmatrix} \tag{12}$$

where

$$\Delta_{\mu\kappa}^{(\pm)}(z) = \frac{1}{2} \left(\frac{1 - \kappa^2 c_{\mathrm{S}}^2(z)}{1 - \kappa^2 \overline{c_{\mathrm{S}}}^2} \pm \frac{\overline{c_{\mathrm{S}}}^2}{c_{\mathrm{S}}^2(z)} \right), \quad \text{and} \quad \begin{bmatrix} \hat{A}_{\mathrm{SH}} \\ \hat{B}_{\mathrm{SH}} \end{bmatrix} = \overline{\mathbf{M}}_{\mathrm{SH}}^{-1} \begin{bmatrix} \hat{v}_y \\ \hat{\sigma}_{yz} \end{bmatrix}. \tag{13}$$

The amplitudes $\hat{A}_{\mathrm{SH}}(\kappa,z,\omega)$ and $\hat{B}_{\mathrm{SH}}(\kappa,z,\omega)$ are those of the upgoing and downgoing modes of the homogenized equation, respectively. Note that, using Eq. (3) (and remembering the discussion of Section 2.3), we have

$$\Delta_{\mu\kappa}^{(\pm)}(z)=\frac{1}{2}\left(1\pm 1+\epsilon\nu(z)\left(\frac{\kappa^2\overline{c_{\mathrm{S}}}^2}{1-\kappa^2\overline{c_{\mathrm{S}}}^2}\pm 1\right)\right). \tag{14}$$

3.2. Recentering of the modes

The second step consists in centering the modes, that is to say writing Eq. (12) in terms of the Fourier transforms (in time) of $a_{\mathrm{SH}}(\kappa,z,t)=A_{\mathrm{SH}}(\kappa,z,t-z/\overline{c_{\mathrm{S}\kappa}})$ and $b_{\mathrm{SH}}(\kappa,z,t)=B_{\mathrm{SH}}(\kappa,z,t+z/\overline{c_{\mathrm{S}\kappa}})$ in a reference frame following an initial pulse in the homogenized medium. In the frequency domain, this yields

$$\frac{d}{dz}\begin{bmatrix}\hat{a}_{\mathrm{SH}}\\ \hat{b}_{\mathrm{SH}}\end{bmatrix}=\frac{i\omega}{\epsilon^2\overline{c_{\mathrm{S}\kappa}}}\begin{bmatrix}\Delta_{\mu\kappa}^{(+)}\left(\frac{z}{\epsilon^2}\right)-1 & \Delta_{\mu\kappa}^{(-)}\left(\frac{z}{\epsilon^2}\right)\mathrm{e}^{-2i\omega z/(\overline{c_{\mathrm{S}\kappa}}\epsilon^2)}\\ -\Delta_{\mu\kappa}^{(-)}\left(\frac{z}{\epsilon^2}\right)\mathrm{e}^{2i\omega z/(\overline{c_{\mathrm{S}\kappa}}\epsilon^2)} & 1-\Delta_{\mu\kappa}^{(+)}\left(\frac{z}{\epsilon^2}\right)\end{bmatrix}\begin{bmatrix}\hat{a}_{\mathrm{SH}}\\ \hat{b}_{\mathrm{SH}}\end{bmatrix} \tag{15}$$

Note that when the domain is homogeneous, that is to say $\nu(z)=0$, we observe that $\Delta_{\mu\kappa}^{(+)}=1$ and $\Delta_{\mu\kappa}^{(-)}=0$, so that the right-hand side of the equation vanishes. As expected, this means that incoming up-going and down-going waves are conserved in a homogeneous medium.

Eventually, the system can be written

$$\frac{d}{dz}\begin{bmatrix}\hat{a}_{\mathrm{SH}}\\ \hat{b}_{\mathrm{SH}}\end{bmatrix}=\frac{i\omega}{2\epsilon}\frac{\overline{c_{\mathrm{S}\kappa}}}{\overline{c_{\mathrm{S}}}^2}\nu\left(\frac{z}{\epsilon^2}\right)\begin{bmatrix}1 & -(1-2\kappa^2\overline{c_{\mathrm{S}}}^2)\mathrm{e}^{-2i\omega z/(\overline{c_{\mathrm{S}\kappa}}\epsilon^2)}\\ (1-2\kappa^2\overline{c_{\mathrm{S}}}^2)\mathrm{e}^{2i\omega z/(\overline{c_{\mathrm{S}\kappa}}\epsilon^2)} & -1\end{bmatrix}\begin{bmatrix}\hat{a}_{\mathrm{SH}}\\ \hat{b}_{\mathrm{SH}}\end{bmatrix} \tag{16}$$

3.3. Initial value problem for the propagator matrix

Boundary conditions must be added to Eq. (16). It is assumed throughout that the incident wave enters the slab from below and that no incoming wave arrives from above (see Fig. 1). This means that $\hat{a}_{\mathrm{SH}}(\kappa,z=0,\omega)=1$ and $\hat{b}_{\mathrm{SH}}(\kappa,z=L,\omega)=0$, and that incidentally the transmission and reflection coefficients are defined by $\mathrm{R}_{\mathrm{SH}}=\hat{b}_{\mathrm{SH}}(\kappa,z=0,\omega)$ and $\mathrm{T}_{\mathrm{SH}}=\hat{a}_{\mathrm{SH}}(\kappa,z=L,\omega)$. The third step of the derivation consists in transforming the boundary value problem Eq. (16) into an initial value problem using a propagator technique.

By definition, the propagator matrix $\mathbf{P}^{\epsilon}_{\mathrm{SH}}(\kappa, z, \omega)$ is defined as the solution of the initial value problem (16) with condition in $z = 0$ equal to the identity matrix. This implies that

$$\begin{bmatrix} \hat{a}_{\mathrm{SH}}(z) \\ \hat{b}_{\mathrm{SH}}(z) \end{bmatrix} = \mathbf{P}^{\epsilon}_{\mathrm{SH}}(z) \begin{bmatrix} \hat{a}_{\mathrm{SH}}(z=0) \\ \hat{b}_{\mathrm{SH}}(z=0) \end{bmatrix}, \tag{17}$$

where we have discarded the dependency of all variables on (κ, ω) for clarity. Symmetries of the matrix in Eq. (16) indicate that the propagator can actually be parameterized as

$$\mathbf{P}^{\epsilon}_{\mathrm{SH}}(z) = \begin{bmatrix} \alpha^{\epsilon}_{\mathrm{SH}}(z) & (\beta^{\epsilon}_{\mathrm{SH}}(z))^* \\ \beta^{\epsilon}_{\mathrm{SH}}(z) & (\alpha^{\epsilon}_{\mathrm{SH}}(z))^* \end{bmatrix}, \tag{18}$$

where the star denotes a complex conjugate, and with the additional constraint that $|\alpha^{\epsilon}_{\mathrm{SH}}(z)|^2 - |\beta^{\epsilon}_{\mathrm{SH}}(z)|^2 = 1$. Eq. (17) means in particular that

$$\begin{bmatrix} \mathrm{T}^{\epsilon}_{\mathrm{SH}} \\ 0 \end{bmatrix} = \mathbf{P}^{\epsilon}_{\mathrm{SH}}(L) \begin{bmatrix} 1 \\ \mathrm{R}^{\epsilon}_{\mathrm{SH}} \end{bmatrix}, \quad \mathrm{R}^{\epsilon}_{\mathrm{SH}} = -\frac{\beta^{\epsilon}_{\mathrm{SH}}(L)}{(\alpha^{\epsilon}_{\mathrm{SH}}(L))^*} \quad \text{and} \quad \mathrm{T}^{\epsilon}_{\mathrm{SH}} = \frac{1}{(\alpha^{\epsilon}_{\mathrm{SH}}(L))^*} \tag{19}$$

3.4. Limit problem (small ϵ) for the propagator

Using limit theorems for ODE with stochastic processes as parameters (see Appendix A, as well as more details in [7, Chapter 6]), it is possible to define the limit, for vanishing ϵ, of the sequence of solutions $\mathbf{P}^{\epsilon}_{\mathrm{SH}}(z)$ as a diffusion process. That diffusion process can itself be characterized as the solution of a SDE, driven by random noise modeled as Brownian motion processes. The fourth step of the analysis therefore consists in considering the Eq. (16) for the propagator, in the limit of small ϵ. This yields the coupled SDE limit system for α_{SH} and β_{SH} (which are the limits of $\alpha^{\epsilon}_{\mathrm{SH}}$ and $\beta^{\epsilon}_{\mathrm{SH}}$, respectively):

$$\begin{aligned} \mathrm{d}\alpha_{\mathrm{SH}}(z) = \frac{\omega\overline{c_{\mathrm{S}\kappa}}(\kappa)}{2\overline{c_{\mathrm{S}}}^2} \Bigg(& i\sqrt{\gamma_\kappa(0)}\alpha_{\mathrm{SH}}(z)\mathrm{d}W_0(z) - \left(1 - 2\kappa^2\overline{c_{\mathrm{S}}}^2\right)\sqrt{\frac{\gamma_\kappa(\omega)}{2}}\beta_{\mathrm{SH}}(z)\left(\mathrm{d}W_1(z) + i\mathrm{d}\widetilde{W}_1(z)\right)\Bigg) \\ & - \frac{\omega^2\overline{c_{\mathrm{S}\kappa}}^2}{8\overline{c_{\mathrm{S}}}^4}\left(\gamma_\kappa(0) - \left(1 - 2\kappa^2\overline{c_{\mathrm{S}}}^2\right)^2\gamma_\kappa(\omega) + i\gamma^{(s)}_\kappa(\omega)\right)\alpha_{\mathrm{SH}}(z)\mathrm{d}z \end{aligned} \tag{20}$$

$$\mathrm{d}\beta_{\mathrm{SH}}(z) = \frac{\omega\overline{c_{\mathrm{S}\kappa}}}{2\overline{c_{\mathrm{S}}}^2}\left(-i\sqrt{\gamma_\kappa(0)}\beta_{\mathrm{SH}}(z)\mathrm{d}W_0(z) - \left(1-2\kappa^2\overline{c_{\mathrm{S}}}^2\right)\sqrt{\frac{\gamma_\kappa(\omega)}{2}}\alpha_{\mathrm{SH}}(z)\left(\mathrm{d}W_1(z) - i\mathrm{d}\widetilde{W}_1(z)\right)\right)$$
$$- \frac{\omega^2\overline{c_{\mathrm{S}\kappa}}^2}{8\overline{c_{\mathrm{S}}}^4}\left(\gamma_\kappa(0) - \left(1-2\kappa^2\overline{c_{\mathrm{S}}}^2\right)^2\gamma_\kappa(\omega) - i\gamma_\kappa^{(s)}(\omega)\right)\beta_{\mathrm{SH}}(z)\mathrm{d}z \quad (21)$$

where $W_0(z)$, $W_1(z)$ and $\widetilde{W}_1(z)$ are independent standard Brownian motions, and

$$\gamma_\kappa(\omega) = 2\int_0^{+\infty} C_\nu(z)\cos\left(\frac{2\omega z}{\overline{c_{\mathrm{S}\kappa}}}\right)\mathrm{d}z, \quad \gamma_\kappa^{(s)}(\omega) = 2\int_0^{+\infty} C_\nu(z)\sin\left(\frac{2\omega z}{\overline{c_{\mathrm{S}\kappa}}}\right)\mathrm{d}z. \quad (22)$$

The solution of this SDE system can be approximated numerically, and the transmission coefficient $\mathrm{T}_{\mathrm{SH}}(\kappa,\omega)$ then obtained using Eq. (19), in the limit of small ϵ, where $\mathrm{T}_{\mathrm{SH}}(\kappa,\omega)$ is the limit of $\mathrm{T}_{\mathrm{SH}}^{\epsilon}(\kappa,\omega)$. In this particular scalar case, further computations (see [7, Chapter 7] for details) yield a direct formula in the limit of thick slabs:

$$\lim_{L\to+\infty}\frac{1}{L}\ln\left|\mathrm{T}_{\mathrm{SH}}(\kappa,\omega)\right|^2 = -\frac{1}{L_{\mathrm{SH}}^{\mathrm{loc}}(\kappa,\omega)}, \quad (23)$$

where

$$L_{\mathrm{SH}}^{\mathrm{loc}}(\kappa,\omega) = \frac{4\overline{c_{\mathrm{S}}}^2\left(1-\kappa^2\overline{c_{\mathrm{S}}}^2\right)}{\left(1-2\kappa^2\overline{c_{\mathrm{S}}}^2\right)^2\omega^2\gamma_\kappa(\omega)}. \quad (24)$$

4. Transmission coefficients for P-SV coupled waves

In this section, we consider the coupled system of Eq. (8). Following the same general steps as in the previous section, we obtain the limit equation for the propagator in the case of P-SV coupled waves. The first step is to project Eq. (8) on a basis of eigenmodes of the homogenized medium.

4.1. Projection on a modal basis

As already previewed in Section 2, for such a medium with isotropic layers, the homogenized medium is orthotropic [8] with behavior given by Eq. (4). In order to stay away from inversions of modal orders, and be able to perform the projections unequivocally (see [9] for a description of modes in orthotropic media), we assume that the angle of incidence is small ($\kappa\overline{c_{\mathrm{S}}} \ll 1$). In that case,

one mode is mainly polarized vertically, and identified as quasi-P, and the other is mainly polarized horizontally, and identified as quasi-SV.

At first order in $\kappa\overline{c_{\rm S}}$, the quasi-P-SV modes in a homogeneous orthotropic medium can be written in the matrix form

$$\overline{\mathbf{M}}_{\rm PSV} = \frac{1}{\sqrt{2}}\begin{bmatrix} \overline{\xi_{\rm S}}^{-1/2} & \overline{\xi_{\rm S}}^{-1/2} & 0 & 0 \\ \overline{\xi_{\rm S}}^{1/2} & -\overline{\xi_{\rm S}}^{1/2} & 0 & 0 \\ 0 & 0 & \overline{\xi_{\rm P}}^{-1/2} & \overline{\xi_{\rm P}}^{-1/2} \\ 0 & 0 & \overline{\xi_{\rm P}}^{1/2} & -\overline{\xi_{\rm P}}^{1/2} \end{bmatrix} + \frac{\kappa\overline{c_{\rm S}}}{\sqrt{2}}\begin{bmatrix} 0 & 0 & \frac{1}{\overline{\alpha}}\overline{\xi_{\rm P}}^{-1/2} & -\frac{1}{\overline{\alpha}}\overline{\xi_{\rm P}}^{-1/2} \\ 0 & 0 & 2\overline{\alpha}\overline{\xi_{\rm P}}^{1/2} & 2\overline{\alpha}\overline{\xi_{\rm P}}^{1/2} \\ -\overline{\xi_{\rm S}}^{-1/2} & \overline{\xi_{\rm S}}^{-1/2} & 0 & 0 \\ -2\overline{\xi_{\rm S}}^{1/2} & -2\overline{\xi_{\rm S}}^{1/2} & 0 & 0 \end{bmatrix} + \mathcal{O}((\kappa\overline{c_{\rm S}})^2), \quad (25)$$

where $\overline{\alpha} = \overline{c_{\rm S}}/\overline{c_{\rm P}}$, $\overline{\xi_{\rm S}} = \rho\overline{c_{\rm S}}$ and $\overline{\xi_{\rm P}} = \rho\overline{c_{\rm P}}$. As expected, at vertical incidence, $\kappa\overline{c_{\rm S}} = 0$, the modes completely decouple and we retrieve separated P and S modes. The inverse matrix is

$$\overline{\mathbf{M}}^{-1}_{\rm PSV} = \frac{1}{\sqrt{2}}\begin{bmatrix} \overline{\xi_{\rm S}}^{1/2} & \overline{\xi_{\rm S}}^{-1/2} & 0 & 0 \\ \overline{\xi_{\rm S}}^{1/2} & -\overline{\xi_{\rm S}}^{-1/2} & 0 & 0 \\ 0 & 0 & \overline{\xi_{\rm P}}^{1/2} & \overline{\xi_{\rm P}}^{-1/2} \\ 0 & 0 & \overline{\xi_{\rm P}}^{1/2} & -\overline{\xi_{\rm P}}^{-1/2} \end{bmatrix} + \frac{\kappa\overline{c_{\rm S}}}{\sqrt{2}}\begin{bmatrix} 0 & 0 & -2\overline{\xi_{\rm S}}^{1/2} & -\overline{\xi_{\rm S}}^{-1/2} \\ 0 & 0 & 2\overline{\xi_{\rm S}}^{1/2} & -\overline{\xi_{\rm S}}^{-1/2} \\ 2\overline{\alpha}\overline{\xi_{\rm P}}^{1/2} & \frac{1}{\overline{\alpha}}\overline{\xi_{\rm P}}^{-1/2} & 0 & 0 \\ -2\overline{\alpha}\overline{\xi_{\rm P}}^{1/2} & \frac{1}{\overline{\alpha}}\overline{\xi_{\rm P}}^{-1/2} & 0 & 0 \end{bmatrix} + \mathcal{O}((\kappa\overline{c_{\rm S}})^2), \quad (26)$$

and projection of Eq. (8) onto the modes of Eq. (25) yields

$$\frac{d}{dz}\begin{bmatrix} \hat{A}_{\rm SV} \\ \hat{B}_{\rm SV} \\ \hat{A}_{\rm P} \\ \hat{B}_{\rm P} \end{bmatrix} = \frac{i\omega}{\epsilon^2\overline{c_{\rm S}}}\mathbf{H}_{\rm PSV}(z)\begin{bmatrix} \hat{A}_{\rm SV} \\ \hat{B}_{\rm SV} \\ \hat{A}_{\rm P} \\ \hat{B}_{\rm P} \end{bmatrix}, \quad \text{where} \quad \begin{bmatrix} \hat{A}_{\rm SV} \\ \hat{B}_{\rm SV} \\ \hat{A}_{\rm P} \\ \hat{B}_{\rm P} \end{bmatrix} = \overline{\mathbf{M}}^{-1}_{\rm PSV}\begin{bmatrix} \hat{v}_x \\ \hat{\sigma}_{xz} \\ \hat{v}_z \\ \hat{\sigma}_{zz} \end{bmatrix}, \quad (27)$$

and

$$\mathbf{H}_{\mathrm{PSV}}(z) = \begin{bmatrix} \Delta_\mu^{(+)}\left(\frac{z}{\epsilon^2}\right) & \Delta_\mu^{(-)}\left(\frac{z}{\epsilon^2}\right) & 0 & 0 \\ -\Delta_\mu^{(-)}\left(\frac{z}{\epsilon^2}\right) & -\Delta_\mu^{(+)}\left(\frac{z}{\epsilon^2}\right) & 0 & 0 \\ 0 & 0 & \overline{\alpha} & 0 \\ 0 & 0 & 0 & -\overline{\alpha} \end{bmatrix}$$

$$+ \kappa\overline{c_{\mathrm{S}}} \begin{bmatrix} 0 & 0 & \Delta^{(+)}\left(\frac{z}{\epsilon^2}\right) & \Delta^{(-)}\left(\frac{z}{\epsilon^2}\right) \\ 0 & 0 & \Delta^{(-)}\left(\frac{z}{\epsilon^2}\right) & \Delta^{(+)}\left(\frac{z}{\epsilon^2}\right) \\ \Delta^{(+)}\left(\frac{z}{\epsilon^2}\right) & -\Delta^{(-)}\left(\frac{z}{\epsilon^2}\right) & 0 & 0 \\ -\Delta^{(-)}\left(\frac{z}{\epsilon^2}\right) & \Delta^{(+)}\left(\frac{z}{\epsilon^2}\right) & 0 & 0 \end{bmatrix} + \mathcal{O}((\kappa\overline{c_{\mathrm{S}}})^2) \quad (28)$$

where

$$\Delta_\mu^{(\pm)}(z) = \frac{1}{2}\left(1 \pm \frac{\overline{\mu}}{\mu(z)}\right) = \frac{1}{2}\left(1 \pm (1 + \epsilon\nu(z))\right), \quad (29)$$

and

$$\Delta^{(\pm)}(z) = -\sqrt{\overline{\alpha}}\left(1 - \frac{\overline{\mu}}{\mu(z)} \pm \overline{\alpha}\left(1 - \frac{\mu(z)}{\overline{\mu}}\right)\right). \quad (30)$$

with $\lim_{\epsilon\to 0} \Delta^{(\pm)}(z)/\epsilon = \sqrt{\overline{\alpha}}(1 \mp \overline{\alpha})\nu(z)$. Note also that $\Delta_\mu^{(\pm)}$ corresponds to $\Delta_{\mu\kappa}^{(\pm)}$ at vertical incidence $\kappa = 0$.

This last coefficient $\Delta^{(\pm)}$ controls the coupling between P and SV waves. The modal amplitudes $\hat{A}_{\mathrm{SV}}$ and $\hat{B}_{\mathrm{SV}}$ denote right- and left-going modes with quasi-SV polarization and $\hat{A}_{\mathrm{P}}$ and $\hat{B}_{\mathrm{P}}$ denote right- and left-going modes with quasi-P polarization.

4.2. Recentering of the modes

We now perform a change of frame (in space-time) for each of the modes, to follow the main pulses, each with its appropriate direction and velocity:

$$\hat{a}_{\mathrm{SV}}(s,z) = \hat{A}_{\mathrm{SV}}\left(s + \frac{z}{\overline{c_{\mathrm{S}}}}, z\right), \quad \hat{b}_{\mathrm{SV}}(s,z) = \hat{B}_{\mathrm{SV}}\left(s - \frac{z}{\overline{c_{\mathrm{S}}}}, z\right), \quad (31)$$

for the quasi-SV modes, and

$$\hat{a}_{\mathrm{P}}(s,z) = \hat{A}_{\mathrm{P}}\left(s + \frac{z}{\overline{c_{\mathrm{P}}}}, z\right), \quad \hat{b}_{\mathrm{P}}(s,z) = \hat{B}_{\mathrm{P}}\left(s - \frac{z}{\overline{c_{\mathrm{P}}}}, z\right), \quad (32)$$

for the quasi-P modes. These changes of frame imply, in the wavenumber-frequency domain, and separating the equations for the quasi-S modes and quasi-P modes, that, to leading orders in $\kappa\overline{c_{\rm S}}$,

$$\frac{d}{dz}\begin{bmatrix}\hat{a}_{\rm P}\\ \hat{b}_{\rm P}\end{bmatrix} = -\frac{i\omega\kappa}{\epsilon^2}\mathbf{H}^1_{\rm SP}\left(\frac{z}{\epsilon^2}\right)\begin{bmatrix}\hat{a}_{\rm SV}\\ \hat{b}_{\rm SV}\end{bmatrix}, \tag{33}$$

and

$$\frac{d}{dz}\begin{bmatrix}\hat{a}_{\rm SV}\\ \hat{b}_{\rm SV}\end{bmatrix} = \frac{i\omega}{\epsilon^2\overline{c_{\rm S}}}\mathbf{H}^0_{\rm SS}\left(\frac{z}{\epsilon^2}\right)\begin{bmatrix}\hat{a}_{\rm SV}\\ \hat{b}_{\rm SV}\end{bmatrix} - \frac{i\omega\kappa}{\epsilon^2}\mathbf{H}^1_{\rm PS}\left(\frac{z}{\epsilon^2}\right)\begin{bmatrix}\hat{a}_{\rm P}\\ \hat{b}_{\rm P}\end{bmatrix}, \tag{34}$$

where the driving matrices are

$$\mathbf{H}^0_{\rm SS}(z) = \begin{bmatrix}\Delta^{(+)}_\mu(z) - 1 & \Delta^{(-)}_\mu(z)e^{-2i\omega z/\overline{c_{\rm S}}}\\ -\Delta^{(-)}_\mu(z)e^{2i\omega z/\overline{c_{\rm S}}} & 1-\Delta^{(+)}_\mu(z)\end{bmatrix} \tag{35}$$

at the leading order in $\kappa\overline{c_{\rm S}}$, and

$$\mathbf{H}^1_{\rm PS}(z) = \begin{bmatrix}\Delta^{(+)}(z)e^{i\omega z/\delta_c^-} & -\Delta^{(-)}(z)e^{i\omega z/\delta_c^+}\\ -\Delta^{(-)}(z)e^{-i\omega z/\delta_c^+} & \Delta^{(+)}(z)e^{-i\omega z/\delta_c^-}\end{bmatrix} \tag{36}$$

and

$$\mathbf{H}^1_{\rm SP}(z) = \begin{bmatrix}\Delta^{(+)}(z)e^{-i\omega z/\delta_c^-} & \Delta^{(-)}(z)e^{i\omega z/\delta_c^+}\\ \Delta^{(-)}(z)e^{-i\omega z/\delta_c^+} & \Delta^{(+)}(z)e^{i\omega z/\delta_c^-}\end{bmatrix} \tag{37}$$

at the following order in $\kappa\overline{c_{\rm S}}$, and where we introduced the harmonic average and difference of velocities:

$$\frac{1}{\delta_c^\pm} = \frac{1}{\overline{c_{\rm S}}} \pm \frac{1}{\overline{c_{\rm P}}}. \tag{38}$$

The harmonic average is always of the order of magnitude of the P-wave velocity $\overline{c_{\rm P}}$, however the harmonic difference may become very small or very large depending on the material. In geophysics, we often observe $\overline{c_{\rm P}} = 2\overline{c_{\rm S}}$ so that $\delta_c^+ = \overline{c_{\rm P}}/3 = 2\overline{c_{\rm S}}/3$ and $\delta_c^- = \overline{c_{\rm P}}/3 = 2\overline{c_{\rm S}}$. Since $\overline{c_{\rm P}} \geq \overline{c_{\rm S}}$, we also have the general ordering $0 \leq \delta_c^+ \leq \min(\overline{c_{\rm P}}/2, \overline{c_{\rm S}}) \leq \overline{c_{\rm S}} \leq \delta_c^-$.

Note that, at vertical incidence, the quasi-P modes are unmodified during their propagation in the slab. This is related to the choice of homogeneous P-wave modulus, and is not true when this modulus is heterogeneous (see Appendix B for the precise formulas). Note also that the matrix $\mathbf{H}^0_{\rm SS}$ is the same

that appeared for the propagation of SH waves at normal incidence (see for instance Eq. (15) with $\kappa = 0$).

Expanding the solutions in $\kappa\overline{c_{\mathrm{S}}}$ as $\hat{a}_i = \hat{a}_i^0 + \kappa\overline{c_{\mathrm{S}}}\hat{a}_i^1 + \mathcal{O}((\kappa\overline{c_{\mathrm{S}}})^2)$ et $\hat{b}_i = \hat{b}_i^0 + \kappa\overline{c_{\mathrm{S}}}\hat{b}_i^1 + \mathcal{O}((\kappa\overline{c_{\mathrm{S}}})^2)$ (where i represents either P or SV), we obtain that

$$\frac{d}{dz}\begin{bmatrix}\hat{a}_{\mathrm{P}}^0\\ \hat{b}_{\mathrm{P}}^0\end{bmatrix} = 0, \tag{39}$$

and

$$\frac{d}{dz}\begin{bmatrix}\hat{a}_{\mathrm{P}}^1\\ \hat{b}_{\mathrm{P}}^1\end{bmatrix} = -\frac{i\omega}{\epsilon^2\overline{c_{\mathrm{S}}}}\mathbf{H}_{\mathrm{SP}}^1\left(\frac{z}{\epsilon^2}\right)\begin{bmatrix}\hat{a}_{\mathrm{SV}}^0\\ \hat{b}_{\mathrm{SV}}^0\end{bmatrix}, \tag{40}$$

for the quasi-P mode, and

$$\frac{d}{dz}\begin{bmatrix}\hat{a}_{\mathrm{SV}}^0\\ \hat{b}_{\mathrm{SV}}^0\end{bmatrix} = \frac{i\omega}{\epsilon^2\overline{c_{\mathrm{S}}}}\mathbf{H}_{\mathrm{SS}}^0\left(\frac{z}{\epsilon^2}\right)\begin{bmatrix}\hat{a}_{\mathrm{SV}}^0\\ \hat{b}_{\mathrm{SV}}^0\end{bmatrix}, \tag{41}$$

and

$$\frac{d}{dz}\begin{bmatrix}\hat{a}_{\mathrm{SV}}^1\\ \hat{b}_{\mathrm{SV}}^1\end{bmatrix} = \frac{i\omega}{\epsilon^2\overline{c_{\mathrm{S}}}}\mathbf{H}_{\mathrm{SS}}^0\left(\frac{z}{\epsilon^2}\right)\begin{bmatrix}\hat{a}_{\mathrm{SV}}^1\\ \hat{b}_{\mathrm{SV}}^1\end{bmatrix} - \frac{i\omega}{\epsilon^2\overline{c_{\mathrm{S}}}}\mathbf{H}_{\mathrm{PS}}^1\left(\frac{z}{\epsilon^2}\right)\begin{bmatrix}\hat{a}_{\mathrm{P}}^0\\ \hat{b}_{\mathrm{P}}^0\end{bmatrix} \tag{42}$$

for the quasi-SV modes.

We recognize that there are actually two independent systems:

$$\frac{d}{dz}\begin{bmatrix}\hat{a}_{\mathrm{P}}^0\\ \hat{b}_{\mathrm{P}}^0\\ \hat{a}_{\mathrm{SV}}^1\\ \hat{b}_{\mathrm{SV}}^1\end{bmatrix} = \frac{i\omega}{\epsilon^2\overline{c_{\mathrm{S}}}}\begin{bmatrix}\mathbf{0} & \mathbf{0}\\ -\mathbf{H}_{\mathrm{PS}}^1\left(\frac{z}{\epsilon^2}\right) & \mathbf{H}_{\mathrm{SS}}^0\left(\frac{z}{\epsilon^2}\right)\end{bmatrix}\begin{bmatrix}\hat{a}_{\mathrm{P}}^0\\ \hat{b}_{\mathrm{P}}^0\\ \hat{a}_{\mathrm{SV}}^1\\ \hat{b}_{\mathrm{SV}}^1\end{bmatrix}. \tag{43}$$

and

$$\frac{d}{dz}\begin{bmatrix}\hat{a}_{\mathrm{SV}}^0\\ \hat{b}_{\mathrm{SV}}^0\\ \hat{a}_{\mathrm{P}}^1\\ \hat{b}_{\mathrm{P}}^1\end{bmatrix} = \frac{i\omega}{\epsilon^2\overline{c_{\mathrm{S}}}}\begin{bmatrix}\mathbf{H}_{\mathrm{SS}}^0\left(\frac{z}{\epsilon^2}\right) & \mathbf{0}\\ -\mathbf{H}_{\mathrm{SP}}^1\left(\frac{z}{\epsilon^2}\right) & \mathbf{0}\end{bmatrix}\begin{bmatrix}\hat{a}_{\mathrm{SV}}^0\\ \hat{b}_{\mathrm{SV}}^0\\ \hat{a}_{\mathrm{P}}^1\\ \hat{b}_{\mathrm{P}}^1\end{bmatrix}. \tag{44}$$

so we will treat them separately, respectively in Sections 4.3 and 4.4.

155 *4.3. Initial value problem and limit problem for the propagator of Eq. (43)*

4.3.1. Initial value problem for the propagator of Eq. (43)

We observe that $(\mathbf{H}^0_{\mathrm{SS}})^{\dagger *} = -\mathbf{H}^0_{\mathrm{SS}}$ and $(\mathbf{H}^1_{\mathrm{PS}})^{\dagger *} = \mathbf{H}^1_{\mathrm{PS}}$, where the dagger $\dagger$ represents the inversion of lines and columns. Note that the dagger is different from the classical transpose operator. For instance, for a general 2×2 matrix, we have

$$\begin{bmatrix} a_{11} & a_{12} \\ a_{21} & a_{22} \end{bmatrix}^{\dagger} = \begin{bmatrix} a_{22} & a_{21} \\ a_{12} & a_{11} \end{bmatrix}, \quad \text{while} \quad \begin{bmatrix} a_{11} & a_{12} \\ a_{21} & a_{22} \end{bmatrix}^{T} = \begin{bmatrix} a_{11} & a_{21} \\ a_{12} & a_{22} \end{bmatrix}. \tag{45}$$

Thanks to that observation and the particular form of Eq. (43), the corresponding propagator is necessarily of the form

$$\mathbf{P}^{\epsilon}_{\mathrm{P}}(z) = \begin{bmatrix} 1 & 0 & 0 & 0 \\ 0 & 1 & 0 & 0 \\ \alpha^{0,\epsilon}_{\mathrm{P}}(z) & -(\beta^{0,\epsilon}_{\mathrm{P}}(z))^* & \alpha^{1,\epsilon}_{\mathrm{SV}}(z) & (\beta^{1,\epsilon}_{\mathrm{SV}}(z))^* \\ \beta^{0,\epsilon}_{\mathrm{P}}(z) & -(\alpha^{0,\epsilon}_{\mathrm{P}}(z))^* & \beta^{1,\epsilon}_{\mathrm{SV}}(z) & (\alpha^{1,\epsilon}_{\mathrm{SV}}(z))^* \end{bmatrix}. \tag{46}$$

Using Jacobi formula, we also have that

$$\frac{d\mathrm{det}\mathbf{P}^{\epsilon}_{\mathrm{P}}}{dz} = \mathrm{det}\mathbf{P}^{\epsilon}_{\mathrm{P}}\mathrm{Tr}\left((\mathbf{P}^{\epsilon}_{\mathrm{P}})^{-1}\frac{d}{dz}\mathbf{P}^{\epsilon}_{\mathrm{P}}\right) = 0, \tag{47}$$

which imposes an additional constraint on the parameters of the propagator matrix: the determinant of the propagator $\mathbf{P}^{\epsilon}_{\mathrm{P}}$ must be a constant. Since its value in $z = 0$ is given, we have that $|\alpha^{1,\epsilon}_{\mathrm{SV}}(z)|^2 - |\beta^{1,\epsilon}_{\mathrm{SV}}(z)|^2 = 1$.

Assuming an incoming P-polarized wave, the boundary conditions for that system read

$$\begin{bmatrix} \mathrm{T}^{0,\epsilon}_{\mathrm{PP}} \\ 0 \\ \mathrm{T}^{1,\epsilon}_{\mathrm{PS}} \\ 0 \end{bmatrix} = \mathbf{P}^{\epsilon}_{\mathrm{P}}(L) \begin{bmatrix} 1 \\ \mathrm{R}^{0,\epsilon}_{\mathrm{PP}} \\ 0 \\ \mathrm{R}^{1,\epsilon}_{\mathrm{PS}} \end{bmatrix}, \tag{48}$$

which implies

$$\mathrm{T}^{0,\epsilon}_{\mathrm{PP}} = 1, \quad \mathrm{R}^{0,\epsilon}_{\mathrm{PP}} = 0, \quad \mathrm{R}^{1,\epsilon}_{\mathrm{PS}} = -\frac{\beta^{0,\epsilon}_{\mathrm{P}}}{(\alpha^{1,\epsilon}_{\mathrm{SV}})^*} \quad \text{and} \quad \mathrm{T}^{1,\epsilon}_{\mathrm{PS}} = \alpha^{0,\epsilon}_{\mathrm{P}} - \beta^{0,\epsilon}_{\mathrm{P}}\left(\frac{\beta^{1,\epsilon}_{\mathrm{SV}}}{\alpha^{1,\epsilon}_{\mathrm{SV}}}\right)^*. \tag{49}$$

4.3.2. Limit problem (small ϵ) for the propagator of Eq. (43)

The definition of the propagator in Eq. (46) and Eq. (43) means that the propagator verifies

$$\frac{\mathrm{d}}{\mathrm{d}z}\mathbf{P}_{\mathrm{P}}^{\epsilon}\left(z\right)=\frac{1}{\epsilon}\mathbf{F}_{\mathbf{P}}\left(\mathbf{P}_{\mathrm{P}}^{\epsilon}\left(z\right),\nu\left(\frac{z}{\epsilon^{2}}\right),\frac{z}{\epsilon^{2}}\right) \tag{50}$$

where

$$\begin{aligned}\mathbf{F}_{\mathbf{P}}\left(\mathbf{X},\Omega,y\right)=&\frac{\omega}{2\overline{c_{\mathrm{S}}}}\Omega\left[\mathbf{h_0}+\sin\left(\frac{2\omega y}{\overline{c_{\mathrm{S}}}}\right)\mathbf{h_1}+\cos\left(\frac{2\omega y}{\overline{c_{\mathrm{S}}}}\right)\mathbf{h_2}\right]\mathbf{X}\\&-\frac{\omega}{\overline{c_{\mathrm{S}}}}\Omega\sqrt{\overline{\alpha}}\left[-\left(1+\overline{\alpha}\right)\left(\sin\left(\frac{\omega y}{\delta_{c}^{+}}\right)\mathbf{h_3}+\cos\left(\frac{\omega y}{\delta_{c}^{+}}\right)\mathbf{h_4}\right)\right.\\&\left.+\left(1-\overline{\alpha}\right)\left(-\sin\left(\frac{\omega y}{\delta_{c}^{-}}\right)\mathbf{h_5}+\cos\left(\frac{\omega y}{\delta_{c}^{-}}\right)\mathbf{h_6}\right)\right]\mathbf{X}\end{aligned} \tag{51}$$

and

$$\begin{aligned}\mathbf{h_0}=\begin{bmatrix}\mathbf{0_2}&\mathbf{0_2}\\\mathbf{0_2}&i\boldsymbol{\sigma}_3\end{bmatrix},\quad\mathbf{h_1}=\begin{bmatrix}\mathbf{0_2}&\mathbf{0_2}\\\mathbf{0_2}&-\boldsymbol{\sigma}_1\end{bmatrix},\quad\mathbf{h_2}=\begin{bmatrix}\mathbf{0_2}&\mathbf{0_2}\\\mathbf{0_2}&\boldsymbol{\sigma}_2\end{bmatrix},\quad\mathbf{h_3}=\begin{bmatrix}\mathbf{0_2}&\mathbf{0_2}\\-i\boldsymbol{\sigma}_2&\mathbf{0_2}\end{bmatrix},\\\mathbf{h_4}=\begin{bmatrix}\mathbf{0_2}&\mathbf{0_2}\\i\boldsymbol{\sigma}_1&\mathbf{0_2}\end{bmatrix},\quad\mathbf{h_5}=\begin{bmatrix}\mathbf{0_2}&\mathbf{0_2}\\-\boldsymbol{\sigma}_3&\mathbf{0_2}\end{bmatrix},\quad\mathbf{h_6}=\begin{bmatrix}\mathbf{0_2}&\mathbf{0_2}\\i\mathbf{I_2}&\mathbf{0_2}\end{bmatrix}\end{aligned} \tag{52}$$

where the $\boldsymbol{\sigma}_1$, $\boldsymbol{\sigma}_2$ and $\boldsymbol{\sigma}_3$ denote the Pauli spins :

$$\boldsymbol{\sigma}_1=\begin{bmatrix}0&1\\1&0\end{bmatrix},\quad\boldsymbol{\sigma}_2=\begin{bmatrix}0&-i\\i&0\end{bmatrix},\quad\boldsymbol{\sigma}_3=\begin{bmatrix}1&0\\0&-1\end{bmatrix}. \tag{53}$$

Following the same limit theorems for ODE as earlier (see [7, Chapter 6] and Appendix A), in the limit of small ϵ, the solution $\mathbf{P}_{\mathrm{P}}^{\epsilon}(z)$ of Eq. (50) converges to the solution $\mathbf{P}_{\mathrm{P}}(z)$ of the following stochastic differential equation:

$$\begin{aligned}\mathrm{d}\mathbf{P}_{\mathrm{P}}=&\frac{\omega\sqrt{\gamma\left(0\right)}}{2\overline{c_{\mathrm{S}}}}\mathbf{h}_0\mathbf{P}_{\mathrm{P}}\circ\mathrm{d}W_0\left(z\right)+\frac{\omega\sqrt{\gamma\left(\omega\right)}}{2\sqrt{2}\overline{c_{\mathrm{S}}}}\left(\mathbf{h}_1\mathbf{P}_{\mathrm{P}}\circ\mathrm{d}W_1\left(z\right)+\mathbf{h}_2\mathbf{P}_{\mathrm{P}}\circ\mathrm{d}\tilde{W}_1\left(z\right)\right)\\&+\frac{\omega}{\sqrt{2}\overline{c_{\mathrm{S}}}}\left(1+\overline{\alpha}\right)\sqrt{\overline{\alpha}\gamma_{+}\left(\omega\right)}\left(\mathbf{h}_3\mathbf{P}_{\mathrm{P}}\circ\mathrm{d}W_2\left(z\right)+\mathbf{h}_4\mathbf{P}_{\mathrm{P}}\circ\mathrm{d}\tilde{W}_2\left(z\right)\right)\\&+\frac{\omega}{\sqrt{2}\overline{c_{\mathrm{S}}}}\left(1-\overline{\alpha}\right)\sqrt{\overline{\alpha}\gamma_{-}\left(\omega\right)}\left(\mathbf{h}_5\mathbf{P}_{\mathrm{P}}\circ\mathrm{d}W_3\left(z\right)-\mathbf{h}_6\mathbf{P}_{\mathrm{P}}\circ\mathrm{d}\tilde{W}_3\left(z\right)\right)\\&-\frac{\gamma^{(s)}(\omega)\omega^{2}}{8\overline{c_{\mathrm{S}}}^{2}}\mathbf{h}_0\mathbf{P}_{\mathrm{P}}\mathrm{d}z\end{aligned} \tag{54}$$

where $W_0(z)$, $W_1(z)$, $\widetilde{W}_1(z)$, $W_2(z)$, $\widetilde{W}_2(z)$, $W_3(z)$ and $\widetilde{W}_3(z)$ are independent standard Brownian motions, and the correlations are

$$\begin{aligned}
\gamma(\omega) &= 2\int_0^{+\infty} C_\nu(z)\cos\left(\frac{2\omega z}{\overline{c_{\mathrm{S}}}}\right)\mathrm{d}z, \quad \gamma^{(s)}(\omega) = 2\int_0^{+\infty} C_\nu(z)\sin\left(\frac{2\omega z}{\overline{c_{\mathrm{S}}}}\right)\mathrm{d}z,\\
\gamma_\pm(\omega) &= 2\int_0^{+\infty} C_\nu(z)\cos\left(\frac{\omega z}{\delta_c^\pm}\right)\mathrm{d}z, \quad \gamma_\pm^{(s)}(\omega) = 2\int_0^{+\infty} C_\nu(z)\sin\left(\frac{\omega z}{\delta_c^\pm}\right)\mathrm{d}z
\end{aligned} \tag{55}$$

4.4. Initial value problem and limit problem for the propagator of Eq. (44)

4.4.1. Initial value problem for the propagator of Eq. (44)

Observing that $(\mathbf{H}^0_{\mathrm{SS}})^{\dagger *} = -\mathbf{H}^0_{\mathrm{SS}}$ and $(\mathbf{H}^1_{\mathrm{SP}})^{\dagger *} = \mathbf{H}^1_{\mathrm{SP}}$, and thanks to the particular form of Eq. (44), the corresponding propagator is necessarily of the form

$$\mathbf{P}^\epsilon_{\mathrm{SV}}(z) = \begin{bmatrix} \alpha^{0,\epsilon}_{\mathrm{SV}}(z) & (\beta^{0,\epsilon}_{\mathrm{SV}}(z))^* & 0 & 0\\ \beta^{0,\epsilon}_{\mathrm{SV}}(z) & (\alpha^{0,\epsilon}_{\mathrm{SV}}(z))^* & 0 & 0\\ \alpha^{1,\epsilon}_{\mathrm{P}}(z) & -(\beta^{1,\epsilon}_{\mathrm{P}}(z))^* & 1 & 0\\ \beta^{1,\epsilon}_{\mathrm{P}}(z) & -(\alpha^{1,\epsilon}_{\mathrm{P}}(z))^* & 0 & 1 \end{bmatrix}. \tag{56}$$

Jacobi formula also implies the additional condition $|\alpha^{0,\epsilon}_{\mathrm{SV}}(z)|^2 - |\beta^{0,\epsilon}_{\mathrm{SV}}(z)|^2 = 1$.

Finally, assuming an SV-polarized incoming wave, the boundary conditions for that system read

$$\begin{bmatrix} \mathrm{T}^{0,\epsilon}_{\mathrm{SS}}\\ 0\\ \mathrm{T}^{1,\epsilon}_{\mathrm{SP}}\\ 0 \end{bmatrix} = \mathbf{P}_{\mathrm{SV}}(L)\begin{bmatrix} 1\\ \mathrm{R}^{0,\epsilon}_{\mathrm{SS}}\\ 0\\ \mathrm{R}^{1,\epsilon}_{\mathrm{SP}} \end{bmatrix}, \tag{57}$$

which implies

$$\mathrm{T}^{0,\epsilon}_{\mathrm{SS}} = \frac{1}{(\alpha^{0,\epsilon}_{\mathrm{SV}})^*}, \quad \mathrm{R}^{0,\epsilon}_{\mathrm{SS}} = -\frac{\beta^{0,\epsilon}_{\mathrm{SV}}}{(\alpha^{0,\epsilon}_{\mathrm{SV}})^*}, \tag{58}$$

and

$$\mathrm{R}^{1,\epsilon}_{\mathrm{SP}} = -\beta^{1,\epsilon}_{\mathrm{P}} - (\alpha^{1,\epsilon}_{\mathrm{P}})^*\frac{\beta^{0,\epsilon}_{\mathrm{SV}}}{(\alpha^{0,\epsilon}_{\mathrm{SV}})^*} \quad \mathrm{T}^{1,\epsilon}_{\mathrm{SP}} = \alpha^{1,\epsilon}_{\mathrm{P}} + (\beta^{1,\epsilon}_{\mathrm{P}})^*\frac{\beta^{0,\epsilon}_{\mathrm{SV}}}{(\alpha^{0,\epsilon}_{\mathrm{SV}})^*}. \tag{59}$$

4.4.2. Limit problem (small ϵ) for the propagator of Eq. (44)

Following the same method as above, the propagator in Eq. (56) and Eq. (44) mean that the propagator verifies the general form Eq. (50) where

$$\begin{aligned}\mathbf{F_P}\left(\mathbf{X},\Omega,y\right) = \frac{\omega}{2\overline{c_{\mathrm{S}}}}\Omega\left[\mathbf{h_0}^{\dagger} + \sin\left(\frac{2\omega y}{\overline{c_{\mathrm{S}}}}\right)\mathbf{h_1}^{\dagger} + \cos\left(\frac{2\omega y}{\overline{c_{\mathrm{S}}}}\right)\mathbf{h_2}^{\dagger}\right]\mathbf{X} \\ - \frac{\omega}{\overline{c_{\mathrm{S}}}}\Omega\sqrt{\overline{\alpha}}\left[\left(1+\overline{\alpha}\right)\left(\sin\left(\frac{\omega y}{\delta_c^+}\right)\mathbf{h_3} + \cos\left(\frac{\omega y}{\delta_c^+}\right)\mathbf{h_4}\right)\right. \\ \left. + \left(1-\overline{\alpha}\right)\left(\sin\left(\frac{\omega y}{\delta_c^-}\right)\mathbf{h_5} + \cos\left(\frac{\omega y}{\delta_c^-}\right)\mathbf{h_6}\right)\right]\mathbf{X} \quad (60)\end{aligned}$$

and the Pauli spins and $\mathbf{h_i}$ matrices were defined in Eq. (53) and Eq. (52), respectively.

Then, in limit of small ϵ, the solution $\mathbf{P}_{\mathrm{SV}}^{\epsilon}(z)$ of Eq. (50) converges to the solution $\mathbf{P}_{\mathrm{SV}}(z)$ of the following stochastic differential equation:

$$\begin{aligned}\mathrm{d}\mathbf{P}_{\mathrm{SV}} = \frac{\omega\sqrt{\gamma\left(0\right)}}{2\overline{c_{\mathrm{S}}}}\mathbf{h}_0^{\dagger}\mathbf{P}_{\mathrm{SV}}\circ\mathrm{d}W_0\left(z\right) + \frac{\omega\sqrt{\gamma\left(\omega\right)}}{2\sqrt{2}\overline{c_{\mathrm{S}}}}\left(\mathbf{h}_1^{\dagger}\mathbf{P}_{\mathrm{SV}}\circ\mathrm{d}W_1\left(z\right) + \mathbf{h}_2^{\dagger}\mathbf{P}_{\mathrm{SV}}\circ\mathrm{d}\tilde{W}_1\left(z\right)\right) \\ + \frac{\omega}{\sqrt{2}\overline{c_{\mathrm{S}}}}\left(1+\overline{\alpha}\right)\sqrt{\overline{\alpha}\gamma_+\left(\omega\right)}\left(\mathbf{h}_3\mathbf{P}_{\mathrm{SV}}\circ\mathrm{d}W_2\left(z\right) + \mathbf{h}_4\mathbf{P}_{\mathrm{SV}}\circ\mathrm{d}\tilde{W}_2\left(z\right)\right) \\ + \frac{\omega}{\sqrt{2}\overline{c_{\mathrm{S}}}}\left(1-\overline{\alpha}\right)\sqrt{\overline{\alpha}\gamma_-\left(\omega\right)}\left(\mathbf{h}_5\mathbf{P}_{\mathrm{SV}}\circ\mathrm{d}W_3\left(z\right) + \mathbf{h}_6\mathbf{P}_{\mathrm{SV}}\circ\mathrm{d}\tilde{W}_3\left(z\right)\right) \\ - \frac{\gamma^{(s)}(\omega)\omega^2}{8\overline{c_{\mathrm{S}}}^2}\mathbf{h}_0\mathbf{P}_{\mathrm{SV}}\mathrm{d}z \quad (61)\end{aligned}$$

where $W_0(z)$, $W_1(z)$, $\widetilde{W}_1(z)$, $W_2(z)$, $\widetilde{W}_2(z)$, $W_3(z)$ and $\widetilde{W}_3(z)$ are independent standard Brownian motions, and the correlations are defined in Eq. (55).

5. Validation of our proposal with semi-analytical and numerical results.

In this final section, we illustrate the interest of the previous Eq. (54-61), the solution of which can be easily approximated, and propose two validations: one with a semi-analytical formula, and the other with a large-scale numerical simulation. We consider the propagation of an SV-polarized incident wave in a particular randomly-fluctuating layered medium, in which we approximate Eq. (61) and compute the corresponding transmission coefficient, and compare

it to the transmission coefficient obtained (i) from the O'Doherty-Anstey approach [6, 2], and, (ii) from full scale results, obtained solving the wave equation with rapidly fluctuating properties. The first part of this section defines the particular case being considered, describing in particular the mechanical properties of the randomly-fluctuating medium. Then, the numerical scheme used to solve Eq. (61) is introduced (Section 5.2), as well as the O'Doherty-Anstey estimates for transmission coefficients (Section 5.3) and the spectral element solver for the full-scale wave equation (Section 5.4). Finally, comparisons are provided and discussed in Section 5.5.

5.1. Description of the physical case

The random slab of Fig. 1 is considered, with an extension of $L_0 = 5000$ m in the vertical direction, and unbounded in the other two directions. The random slab is embedded between two (deterministic) homogeneous half-spaces. The parameters describing the mechanical properties of the random slab are reported in Table 1: the velocities and density are homogenized properties, and the fluctuations follow a Gaussian correlation model whose correlation length ℓ_c and variance σ_K are also provided in Table 1. The choice of correlation model implies the following power spectrum densities:

$$\gamma\left(\omega\right) = \ell_c \sigma_K^2 e^{-\ell_c^2 \omega^2 \pi / \overline{c_{\mathrm{S}}}^2}, \quad \gamma^{(s)}\left(\omega\right) = \frac{1}{2\sqrt{\pi}} \gamma\left(\omega\right) \operatorname{erfi}\left(\frac{\ell_c \omega \pi}{\overline{c_{\mathrm{S}}}}\right), \tag{62}$$

where erfi is the imaginary error function, and

$$\gamma_{\pm}(\omega) = \ell_c \sigma_K^2 e^{-\ell_c^2 \omega^2 \pi / 4(\delta_c^{\pm})^2} \quad , \gamma_{\pm}^{(s)}\left(\omega\right) = \frac{1}{2\sqrt{\pi}} \gamma_{\pm}\left(\omega\right) \operatorname{erfi}\left(\frac{\ell_c \omega \pi}{2\delta_c^{\pm}}\right). \tag{63}$$

Table 1: Mechanical properties of the medium (for the half-spaces, and homogenized properties of the slab) and parameters of the random fluctuations in the slab.

ρ	$\overline{c_{\mathrm{P}}}$	$\overline{c_{\mathrm{S}}}$	σ_K	ℓ_c
2800 kg/m^3	1750 m/s	1000 m/s	0.3	50 m

The incident wave on the slab is considered to have SV polarization. Three incidences will be considered: vertical incidence $\kappa = 0°$, for which there is no coupling, as well as $\kappa = 5°$ and $\kappa = 10°$.

190 *5.2. Numerical approximation of SDE (our proposal)*

In this part, we describe the numerical scheme used for the approximation of the solution of Eq. (61), namely a Euler-Maruyama scheme. The numerical integration is performed considering independent realizations of the brownian motion jumps [10]. The discrete equations under Îto form are written in Eq. (64-67), where the G_i^n, $n \geq 0$, $0 \leq i \leq 3$ and $\widetilde{G}_i^n$, $n \geq 0$, $1 \leq i \leq 3$, are all independent centered Gaussian random variable with variance equal to the space step $\Delta z = L/N$, assumed to be constant here, and where N is the total number of space steps. The coupled system for $(\alpha_{\mathrm{S}}^0)^n$ and $(\beta_{\mathrm{S}}^0)^n$, $0 \leq n \leq N$, is first solved, with initial conditions $(\alpha_{\mathrm{S}}^0)^0 = 1$ and $(\beta_{\mathrm{S}}^0)^0 = 0$.

$$(\alpha_{\mathrm{S}}^0)^{n+1} = (\alpha_{\mathrm{S}}^0)^n + \frac{\omega}{2\overline{c_{\mathrm{S}}}} \left(i\sqrt{\gamma(0)}(\alpha_{\mathrm{S}}^0)^n G_0^{n+1} - \sqrt{\frac{\gamma(\omega)}{2}}(\beta_{\mathrm{S}}^0)^n \left(G_1^{n+1} + i\widetilde{G}_1^{n+1} \right) \right) - \frac{\omega^2}{8\overline{c_{\mathrm{S}}}^2} \left(\gamma(0) - \gamma(\omega) + i\gamma^{(s)}(\omega) \right) (\alpha_{\mathrm{S}}^0)^n \Delta z, \quad (64)$$

$$(\beta_{\mathrm{S}}^0)^{n+1} = (\beta_{\mathrm{S}}^0)^n - \frac{\omega}{2\overline{c_{\mathrm{S}}}} \left(i\sqrt{\gamma(0)}(\beta_{\mathrm{S}}^0)^n G_0^{n+1} + \sqrt{\frac{\gamma(\omega)}{2}}(\alpha_{\mathrm{S}}^0)^n \left(G_1^{n+1} - i\widetilde{G}_1^{n+1} \right) \right) - \frac{\omega^2}{8\overline{c_{\mathrm{S}}}^2} \left(\gamma(0) - \gamma(\omega) - i\gamma^{(s)}(\omega) \right) (\beta_{\mathrm{S}}^0)^n \Delta z. \quad (65)$$

Then the rest of the equations are solved, for $(\alpha_{\mathrm{P}}^1)^n$ and $(\beta_{\mathrm{P}}^1)^n$, $0 \leq n \leq N$, with initial conditions $(\alpha_{\mathrm{P}}^1)^0 = 0$ and $(\beta_{\mathrm{P}}^1)^0 = 0$, and taking the $(\alpha_{\mathrm{S}}^0)^n$ and $(\beta_{\mathrm{S}}^0)^n$, $0 \leq n \leq N$ as given.

$$(\alpha_{\mathrm{P}}^1)^{n+1} = (\alpha_{\mathrm{P}}^1)^n + \frac{\omega}{\sqrt{2}\overline{c_{\mathrm{S}}}} \left(1 + \overline{\alpha}^2 \right) \sqrt{\overline{\alpha}\gamma_+(\omega)}(\beta_{\mathrm{S}}^0)^n \left(G_2^{n+1} + i\widetilde{G}_2^{n+1} \right) - \frac{\omega}{\sqrt{2}\overline{c_{\mathrm{S}}}} \left(1 - \overline{\alpha}^2 \right) \sqrt{\overline{\alpha}\gamma_-(\omega)}(\alpha_{\mathrm{S}}^0)^n \left(G_3^{n+1} - i\widetilde{G}_3^{n+1} \right) + i\frac{\omega^2}{2\overline{c_{\mathrm{S}}}^2}\gamma_+^{(s)}(\alpha_{\mathrm{S}}^0)^n \Delta z \quad (66)$$

$$(\beta_{\mathrm{P}}^1)^{n+1} = (\beta_{\mathrm{P}}^1)^n - \frac{\omega}{\sqrt{2}\overline{c_{\mathrm{S}}}} \left(1 + \overline{\alpha}^2 \right) \sqrt{\overline{\alpha}\gamma_+(\omega)}(\alpha_{\mathrm{S}}^0)^n \left(G_2^{n+1} - i\widetilde{G}_2^{n+1} \right) + \frac{\omega}{\sqrt{2}\overline{c_{\mathrm{S}}}} \left(1 - \overline{\alpha}^2 \right) \sqrt{\overline{\alpha}\gamma_-(\omega)}(\beta_{\mathrm{S}}^0)^n \left(G_3^{n+1} + i\widetilde{G}_3^{n+1} \right) - i\frac{\omega^2}{2\overline{c_{\mathrm{S}}}^2}\gamma_+^{(s)}(\omega)(\beta_{\mathrm{S}}^0)^n \Delta z \quad (67)$$

After solving these two coupled systems (for each frequency ω), transmission coefficients (see Eq. (58) and Eq. (59)) are computed. In the simulations discussed in Section 5.5, the step $\Delta z = 1.65 \times 10^{-5}$ is used, and 30 realizations are computed for each transmission coefficient by repeating the process 30 times.

5.3. O'Doherty Anstey formula approach [2]

The O'Doherty-Anstey formula for normally-incident acoustic waves, and subsequent refinements (for oblique waves, as well as for elastic waves), are described in detail in [2]. The formula are derived under an hypothesis of small fluctuations of the mechanical parameters, and assuming that the thickness is not too large (of the order of the inverse of the variance of the fluctuations). Following the setting of the Rytov approximation (a Taylor expansion of the phase of the wave field is considered rather than that of the wave field itself), the transmission coefficient is computed as an exponentially-decreasing function of the depth in the slab, whose characteristic length for S-wave is the localization length given by

$$\begin{aligned}\left(L^{\mathrm{loc}}\right)^{-1} = \frac{\omega^2\gamma\left(\omega\right)}{4}\frac{\left(1-8\kappa^2\overline{c_{\mathrm{S}}}^2(1-\kappa^2\overline{c_{\mathrm{S}}}^2)\right)^2}{\overline{c_{\mathrm{S}}}^2(1-\kappa^2\overline{c_{\mathrm{S}}}^2)} \\ + \frac{\omega^2\kappa^2}{\sqrt{1-\kappa^2\overline{c_{\mathrm{S}}}^2}\sqrt{1-\kappa^2\overline{c_{\mathrm{P}}}^2}}\Big[\left(1-2\kappa^2\overline{c_{\mathrm{S}}}^2\right)\sqrt{1-\kappa^2\overline{c_{\mathrm{P}}}^2}\left(\gamma_-\left(\omega\right)-\gamma_+\left(\omega\right)\right) \\ -\overline{\alpha}^2\sqrt{1-\kappa^2\overline{c_{\mathrm{S}}}^2}(1-2\kappa^2\overline{c_{\mathrm{P}}}^2)\left(\gamma_-\left(\omega\right)+\gamma_+\left(\omega\right)\right)\Big] \quad (68)\end{aligned}$$

where the wavenumber is assumed small enough ($\kappa < 1$ and $\kappa < 1/\overline{c_{\mathrm{P}}}$), and the correlation functions $\gamma_+(\omega)$ and $\gamma_-(\omega)$ are given in Eq. (63). When $\kappa = 0$, this formula simplifies to $L^{\mathrm{loc}} = 4\overline{c_{\mathrm{S}}}^2/(\omega^2\gamma(\omega))$, and the formula in Eq. (24) is recovered.

The main issue with this approach is that limited information is provided concerning transfer of energy between different polarization. Losses are accounted for in the incident polarization, but the energy transferred from that incident polarization to the other polarization is not monitored. For instance, in the present case of an incident SV-wave, there is no information on the P-polarized waves, and hence on the SV-to-P transmission coefficient $\mathrm{T_{SP}}(\omega)$.

5.4. Numerical approximation of wave equation

Finally we introduce a full-scale numerical approach, to solve directly the equilibrium Eq. (1), in time and in 3D, based on one realization of the random material properties. The Spectral Element Method is used, which is a high order Finite Element Method with low numerical dispersion and high efficiency [11, 12]. It computes the displacement field at any point in the domain and the transmission coefficient can be estimated from this. More specifically, the implementation used in this study is the SEM3D code, jointly developed by CEA, IPGP, CentraleSupélec and CNRS [13].

As with any Finite Element Method, the computational domain must be bounded, as presented in Fig. 2, where the positions of the receivers, used to estimate the transmission coefficients are also represented. This truncation creates parasitic reflected waves when simulating for an unbounded model (as in our case of interest, see Fig. 1). In our application, the dimensions of the computational domain are chosen to be $6 \times 6 \times 11$ km^3, and we consider free surface conditions at all boundaries. This is deemed enough to minimize the impact of the reflections on wavefields of interest over the simulation time considered. The use of more elaborate boundary conditions (such as Perfectly Match Layers) would also be possible but would have resulted in even higher computational cost (current simulations required 4 hours of computational time on 600 processors, which means close to 2500 hours of CPU time). The solution is approximated on tensorized polynomials (of order 4 in each direction) in each element, and element size is fixed at $h = 27$ m, which ensures that waves at frequencies below 20 Hz are well approximated. Fig. 3 displays a representative map of $c_{\mathrm{S}}(z)$ for one particular realization of the random field described in Section 5.1.

As described in Section 5.1, the incident field is a plane wave, SV-polarized, and inclined (with an angle ψ around the axis $\mathbf{e}_y$). This is created by introducing a series of point-sources, along a plane orthogonal to $\mathbf{e}_{\mathrm{P}} = \sin\psi\,\mathbf{e}_x + \cos\psi\,\mathbf{e}_z$, with separations much smaller than the wavelength, and with directions along $\mathbf{e}_{\mathrm{SV}} = \cos\psi\,\mathbf{e}_x - \sin\psi\,\mathbf{e}_z$. The signal for each of these sources is represented in Fig. 4. It has an almost flat spectrum between 2 Hz and 20 Hz, which makes

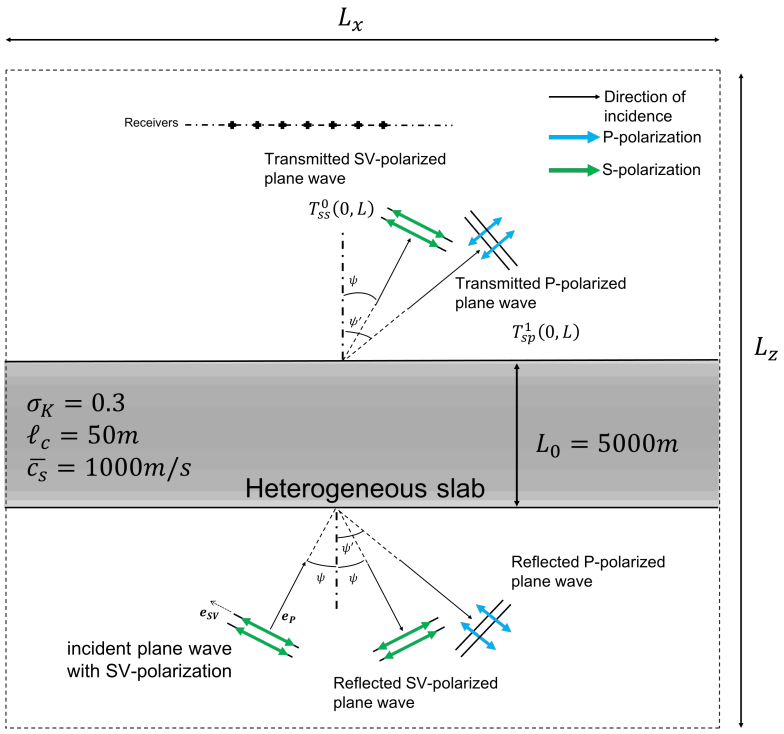

Figure 2: Section of the 3D geometry for SEM3D solver. The dimensions are $L_x = 5$ km, $L_z = 11$ km, and the thickness in the unrepresented dimension is $L_y = 5$ km. There are 1680 receivers and three incidence angles are considered: $\psi = 0°$, $\psi = 5°$ and $\psi = 10°$.

comparisons of transmission coefficients with the other two methods easier in that frequency range. Note that the boundedness of the computational domain means that the plane wave is only partially represented. This translates into parasitic effects at the boundary of the domain, that can be seen for instance in Fig. 5, frame $t = 1$ s, for P-polarization (right column).

The full wavefield is simulated at all times (see Fig. 5 for some snapshots of the components of the velocity field along $\mathbf{e}_{\mathrm{SV}}$ and $\mathbf{e}_{\mathrm{P}}$, respectively). It is observed that there is initially no velocity along $\mathbf{e}_{\mathrm{P}}$ (except a boundary effect along the loading line, note the ten-folds difference in amplitude for the SV-velocity and P-velocity). This P-velocity grows along when the S-wave propagates inside the domain, and propagates with a different direction than the SV-velocity

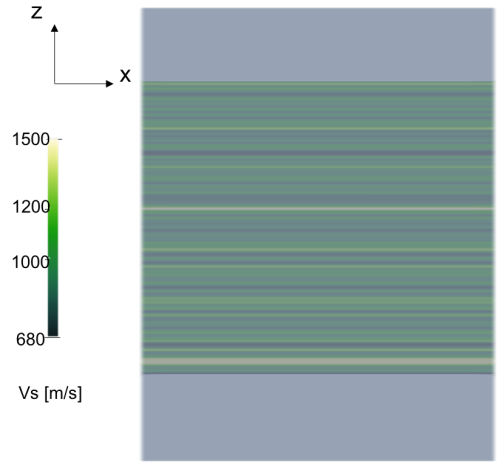

Figure 3: Shear velocity $c_S(\mathbf{x})$ in a section of one realization of the SEM3D model ($\ell_c = 50$ m, $\sigma_K = 0.3\%$ and $L_0 = 5$ km).

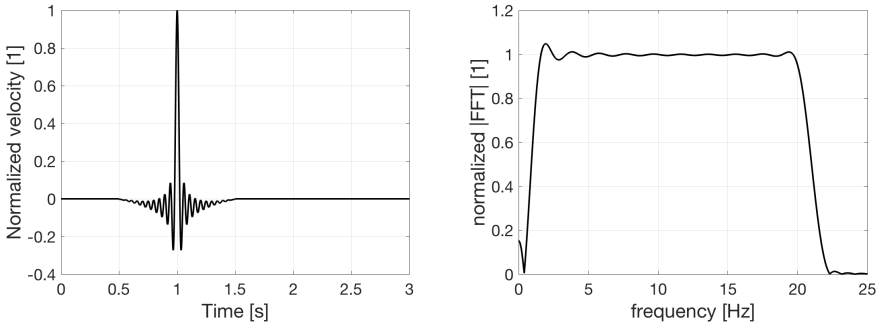

Figure 4: Time signal injected at source point (left) and its associated frequency content (right).

(actually the angle corresponding to the same κ for a P-wave, as predicted by Fresnel equations). In order to compute the transmission coefficients, 1680 receivers are placed regularly on a plane 200 m downstream (see Fig. 2) to measure the signal coming out of the random layer. The results are analyzed in frequency and the spectra are averaged over all receivers in order to remove the influence of local phenomena. Also, to follow the polarization of the wave through the

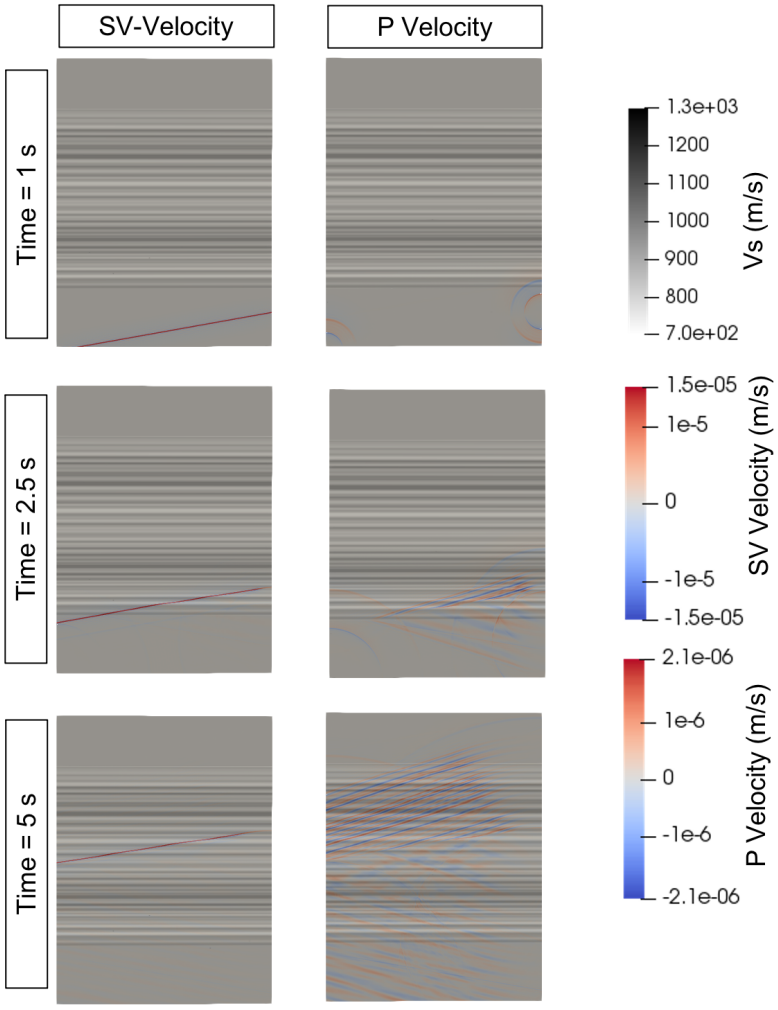

Figure 5: Components of the velocity field along $\mathbf{e}_{\mathrm{SV}}$ (SV-velocity) and $\mathbf{e}_{\mathrm{P}}$ (P-velocity) at several times for an SV-polarized wave with incidence $\psi = 10°$. Note the ten-folds difference in amplitude for the SV-velocity and P-velocity.

propagation, the velocity field is projected in the rotated space ($\mathbf{e}_{\mathrm{SV}}$,$\mathbf{e}_{\mathrm{P}}$).

255 The main advantage of considering these very expensive simulations is that both SV-to-SV and SV-to-P transmission coefficients can be evaluated. How-

ever, comparisons should be done with care because results here correspond to only one realization of the mechanical parameters, contrarily to the previous methods that consider homogenization and predict an average transmission coefficient, expected to be much smoother. To simplify comparisons, three simulations are considered (each for different realizations of the mechanical parameters). Simulating for more realizations appears unnecessarily expensive.

5.5. Transmission coefficients computed with the three different methods

The normal incidence ($\psi = 0°$) is first considered. The transmission coefficients are estimated for the three methods and plotted in Figure 6). In the case of the SEM3D simulations, 3 realizations are plotted, along with the average. For our method, 30 realizations are considered and the average as well as a confidence interval for one standard deviation are plotted. Our approach appears to give results very similar to those of ODA. The full-scale results also compare reasonably well with the others, considering in particular the issues with the boundary conditions in the numerical model.

We then move to higher angles of incidences: $\psi = 5°$ and $\psi = 10°$. The SV-to-SV transmission coefficients $\mathrm{T_{SS}}(\omega)$ are plotted in Fig. 7 and the SV-to-P transmission coefficients $\mathrm{T_{SP}}(\omega)$ are plotted in Fig. 8. Concerning the SV-to-SV transmission, it seems that the observations made for the normal incidence still apply in the low-frequency range (below 10 Hz approximately): all three approaches seem to correspond. At higher frequencies, our approach seems less efficient and cannot predict the decrease in transmission with respect to the normal case. This is most probably due to the hypothesis of small angle of incidence, that could be eventually removed by considering more accurate propagation modes in Eq. (25) (see [14] for instance).

Finally, concerning the SV-to-P transmission coefficients, the ODA does not provide estimates so only the expensive full-scale approach and our approach are available. Given the differences discussed above, comparisons in Fig. 8 seem convincing that our approach can provide accurate prediction of the SV-to-P transmission in a horizontally stratified slab.

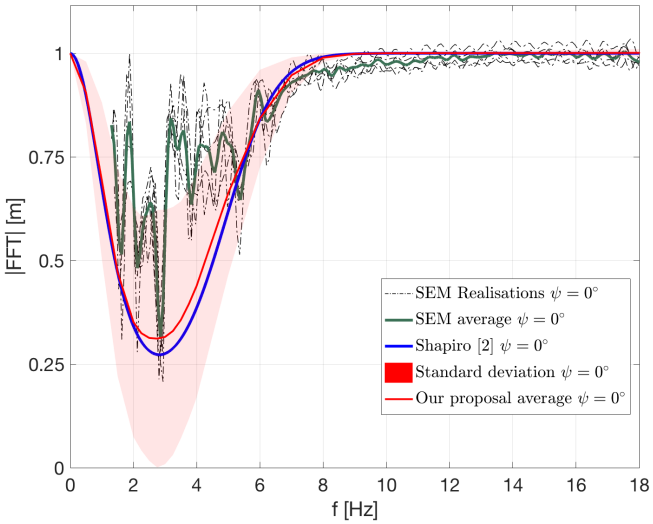

Figure 6: SV-to-SV transmission coefficient $T_{SS}(\omega)$ for normal incidence ($\psi = 0°$): 3 realizations (dashed grey lines) and average (green solid line) computed with the SEM3D approach (Section 5.4), ODA formula (blue line) of Section 5.3, and average (red solid line) plus or minus one standard deviation (pink shade) estimated with 30 realizations of our approach (Section 5.2).

6. Conclusions

In this paper, we have proposed a method to determine the transmission coefficients for an elastic wave propagating at an angle in a horizontally-stratified randomly-fluctuating slab as the solution of a set of coupled stochastic differential equations. Solutions of that set of equations can be easily simulated because small scales of fluctuation of the mechanical properties have been homogenized. The SV-to-SV transmission coefficient obtained with our method compares favorably to the ODA formula [2] and additionally provides the evaluation of the SV-to-P transmission coefficient. The behavior in the higher frequency range could be improved by removing the Taylor expansion in κ. Finally, it would be interesting to try and derive an analytical formula for the elastic case, in the manner of Eq. (23-24).

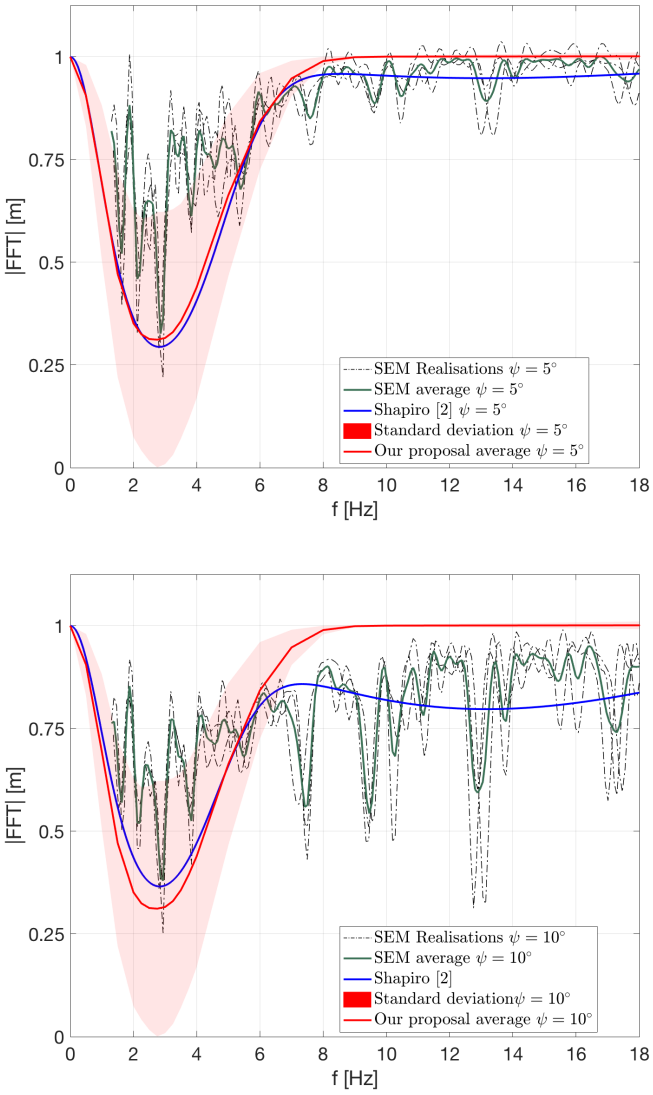

Figure 7: SV-to-SV transmission coefficients $T_{SS}(\omega)$ for incidences $\psi = 5°$ (upper plot) and $\psi = 10°$ (lower plot): 3 realizations (dashed grey lines) and average (green solid line) computed with the SEM3D approach (Section 5.4), ODA formula (blue line) of Section 5.3, and average (red solid line) plus or minus one standard deviation (pink shade) estimated with 30 realizations of our approach (Section 5.2).

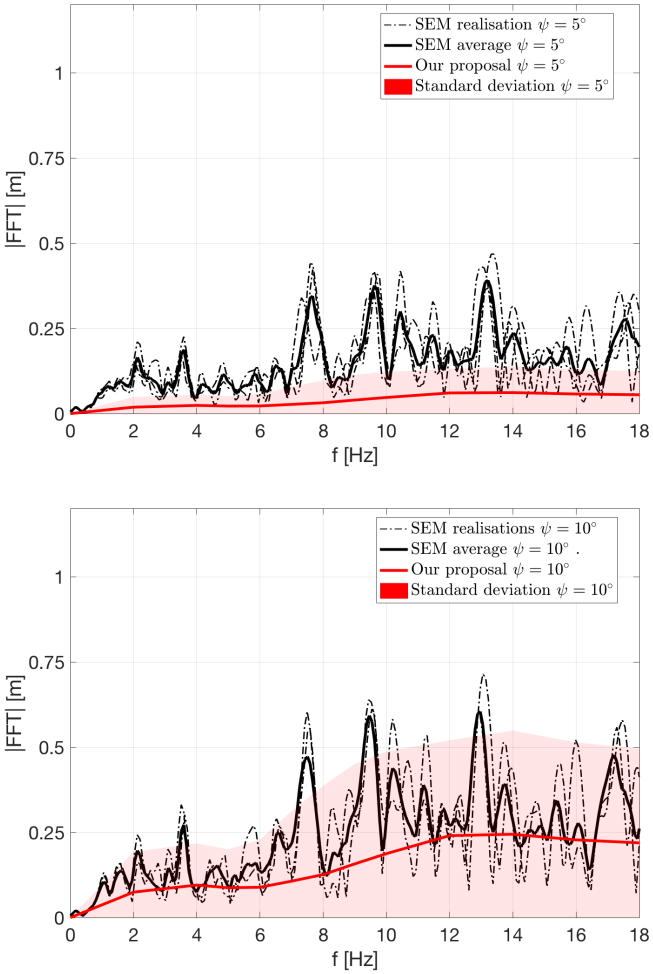

Figure 8: SV-to-P transmission coefficients $T_{SP}(\omega)$ for incidences $\psi = 5°$ (upper plot) and $\psi = 10°$ (lower plot): 3 realizations (dashed grey lines) and average (black solid line) computed with the SEM3D approach (Section 5.4), and average (red solid line) plus or minus one standard deviation (pink shade) estimated with 30 realizations of our approach (Section 5.2).

Acknowledgements

Simulations were performed using open-source and free software SEM3D, a Spectral Element solver jointly developed by MSSMat Laboratory (Centrale-Supélec, CNRS and Université Paris-Saclay), Institut de Physique du Globe de

Paris (Paris Institute of Earth Physics) and the Commissariat à l'Énergie Atomique et aux énergies alternatives (French Atomic Energy Commission), available at https://github.com/sem3d/SEM. This work was performed using HPC resources from the "Mésocentre" computing center of CentraleSupélec, École Normale Supérieure Paris-Saclay and Université Paris-Saclay supported by CNRS and Région Île-de-France (https://mesocentre.universite-paris-saclay.fr/). The authors would also like to thank Cédric Sultan for carefully reading the manuscript and spotting several important typos in the formulas before publication.

References

[1] H. Sato, M. C. Fehler, T. Maeda, Seismic wave propagation and scattering in the heterogeneous earth (2011).

[2] S. A. Shapiro, P. Hubral, Elastic waves in random media: Fundamentals of seismic stratigraphic filtering, Springer Berlin, 1999.

[3] A.-M. Zelenyak, N. Schorer, M. G. Sause, Modeling of ultrasonic wave propagation in composite laminates with realistic discontinuity representation, Ultrasonics 83 (2018) 103–113.

[4] D. G. Aggelis, Wave propagation through engineering materials; assessment and monitoring of structures through non-destructive techniques, Materials and Structures 46 (4) (2013) 519–532.

[5] S. M. Rytov, Y. A. Kravtsov, V. I. Tatarskii, Principles of statistical radiophysics: wave propagation through random media, Springer, 1989.

[6] R. F. O'Doherty, N. A. Anstey, Reflections on amplitudes, Geophysical Prospecting 19 (3) (1971) 430–458. doi:10.1111/j.1365-2478.1971.tb00610.x.

[7] J.-P. Fouque, J. Garnier, G. Papanicolaou, K. Solna, Wave propagation and time reversal in randomly layered media, Vol. 56, Springer Science & Business Media, 2007.

[8] G. E. Backus, Long-wave elastic anisotropy produced by horizontal layering, Journal of Geophysical Research 67 (11) (1962) 4427–4440.

[9] P. Chadwick, Wave propagation in transversely isotropic elastic media-ii. surface waves, Proceedings of the Royal Society of London. A. Mathematical and Physical Sciences 422 (1862) (1989) 67–101.

[10] T. Sauer, Numerical solution of stochastic differential equations in finance, in: Handbook of computational finance, Springer, 2012, pp. 529–550.

[11] D. Komatitsch, J. Tromp, Introduction to the spectral element method for three-dimensional seismic wave propagation, Geophysical journal international 139 (3) (1999) 806–822.

[12] D. Göddeke, D. Komatitsch, M. Möller, Finite and spectral element methods on unstructured grids for flow and wave propagation problems, in: Numerical Computations with GPUs, Springer, 2014, pp. 183–206.

[13] S. Touhami, F. Gatti, F. Lopez-Caballero, R. Cottereau, L. de Abreu Corrêa, L. Aubry, D. Clouteau, Sem3d: A 3d high-fidelity numerical earthquake simulator for broadband (0–10 hz) seismic response prediction at a regional scale, Geosciences 12 (3) (2022) 112.

[14] K. Aki, P. G. Richards, Quantitative seismology: Theory and methods, W. H. Freeman and Company, 1980.

Appendix A. Limit theorem for ODEs with stochastic parameters

We recall here the main theorem that is used in this paper. It is described in more detail, along with a proof in [7]. The main idea is that the limit of a sequence of solutions of ordinary differential equations with random parameters can be described (in the regime that we are interested in) as a diffusion Markov process. The characterization of that diffusion process can then be performed, among other possibilities, as the solution of a stochastic differential equation.

This is the characterization that is proposed in this paper (following [7]). The theorem goes as below.

Theorem 1. *Let the process $X^\epsilon(z)$ be defined by the following system of ordinary differential equations with random parameter:*

$$\frac{dX^\epsilon}{dz} = \frac{1}{\epsilon} F\left(X^\epsilon(z), Y\left(\frac{z}{\epsilon^2}\right), \frac{z}{\epsilon^2}\right), \tag{A.1}$$

starting from $X^\epsilon(0) = x_0 \in \mathbb{R}^d$. We assume that $Y(z)$ is a z-homogeneous Markov ergodic process with generator satisfying the Fredholm alternative. The $\mathbb{R}^d$-valued function $F(x, y, \tau)$ is assumed to be at most linearly growing and smooth in x, to be periodic with period Z_0 with respect to τ, and to satisfy the centering condition $\int_0^{Z_0} \mathbb{E}\left[F\left(x, Y(0), \tau\right)\right] d\tau = 0$, for all x, where $\mathbb{E}[\cdot]$ denotes expectation with respect to the invariant probability distribution of $Y(z)$. Then the random processes $X^\epsilon(z)$ converge in distribution to the diffusion Markov process $X(z)$ with generator

$$\mathcal{L}\phi(x) = \frac{1}{Z_0} \int_0^{Z_0} \int_0^{\infty} \mathbb{E}\left[F\left(x, Y(0), \tau\right) \cdot \nabla_x F\left(x, Y(z), \tau + z\right) \cdot \nabla_x \phi(x)\right] dz d\tau. \tag{A.2}$$

Appendix B. Case of a heterogeneous P-wave modulus

Adding to the fluctuation properties defined for shear modulus Eq. (3), P-wave modulus is considered to randomly fluctuate inside the random slab. This P-wave modulus is modeled as :

$$\frac{1}{K(z)} = \frac{1}{\overline{K}} \left(1 + \nu_K(z)\right), \quad 0 \leq z \leq L, \tag{B.1}$$

where $\nu_K(z)$ satisfies the same properties as $\nu(z)$ (see Eq. (3)) with a given autocovariance $C_K(z)$, its variance $\sigma_K^2 = C_K(0)$, the correlation length $\ell_{c,K} = \int_{\mathbb{R}} C_K(z) dz / \sigma_K^2$ and $\overline{K} = \mathbb{E}[1/K(z)]^{-1}$ the harmonic average. K and μ are

assumed to be independant. Considering $c_{\mathrm{P}}(z)$, Eq. (8) becomes :

$$\frac{d}{dz}\begin{bmatrix}\hat{v}_x\\ \hat{\sigma}_{xz}\\ \hat{v}_z\\ \hat{\sigma}_{zz}\end{bmatrix} = i\omega\begin{bmatrix}0 & (\rho c_{\mathrm{S}}^2)^{-1} & -\kappa & 0\\ \rho(1-4\kappa^2(1-\alpha^2)c_{\mathrm{S}}^2) & 0 & 0 & -\kappa(1-2\alpha^2)\\ -\kappa(1-2\alpha^2) & 0 & 0 & (\rho c_{\mathrm{P}}^2)^{-1}\\ 0 & -\kappa & \rho & 0\end{bmatrix}\begin{bmatrix}\hat{v}_x\\ \hat{\sigma}_{xz}\\ \hat{v}_z\\ \hat{\sigma}_{zz}\end{bmatrix}. \tag{B.2}$$

In this case, the constitutive relation of the two half-spaces is given, for $(\mathbf{x}, z) \in \Omega^- \cup \Omega^+$, by

$$\sigma = \rho\begin{bmatrix}\overline{c_{\mathrm{Ph}}}^2 & \overline{c_{\mathrm{Ph}}}^2 - 2\overline{c_{\mathrm{Sh}}}^2 & \overline{c_{\mathrm{P}}}^2(1-2\overline{\alpha}^2) & 0 & 0 & 0\\ \overline{c_{\mathrm{Ph}}}^2 - 2\overline{c_{\mathrm{Sh}}}^2 & \overline{c_{\mathrm{Ph}}}^2 & \overline{c_{\mathrm{P}}}^2(1-2\overline{\alpha}^2) & 0 & 0 & 0\\ \overline{c_{\mathrm{P}}}^2(1-2\overline{\alpha}^2) & \overline{c_{\mathrm{P}}}^2(1-2\overline{\alpha}^2) & \overline{c_{\mathrm{P}}}^2 & 0 & 0 & 0\\ 0 & 0 & 0 & \overline{c_{\mathrm{S}}}^2 & 0 & 0\\ 0 & 0 & 0 & 0 & \overline{c_{\mathrm{S}}}^2 & 0\\ 0 & 0 & 0 & 0 & 0 & \overline{c_{\mathrm{Sh}}}^2\end{bmatrix}\epsilon \tag{B.3}$$

where the coefficients are :

$$\overline{c_{\mathrm{P}}}^2 = \mathbb{E}\left[\frac{1}{c_{\mathrm{P}}^2(z)}\right]^{-1}, \quad \overline{c_{\mathrm{S}}}^2 = \mathbb{E}\left[\frac{1}{c_{\mathrm{S}}^2(z)}\right]^{-1}, \quad \overline{c_{\mathrm{Sh}}}^2 = \mathbb{E}\left[c_{\mathrm{S}}^2(z)\right], \tag{B.4}$$

and

$$c_{\mathrm{Ph}}^2 = 4c_{\mathrm{Sh}}^2 + c_{\mathrm{P}}^2\left(1-2\overline{\alpha}^2\right)^2 - \frac{4}{\rho}\mathbb{E}\left[\frac{\mu^2(z)}{K(z)}\right], \quad \overline{\alpha}^2 = \mathbb{E}[\alpha(z)^2] \tag{B.5}$$

From this behavior, we can proceed to the projection and the recentering of the modes (see sections 4.1 and 4.2). Then, the asymptotic extension under the assumption of a small angle yields :

$$\frac{d}{dz}\begin{bmatrix}\hat{a}_{\mathrm{S}}^0\\ \hat{b}_{\mathrm{S}}^0\\ \hat{a}_{\mathrm{P}}^1\\ \hat{b}_{\mathrm{P}}^1\\ \hat{a}_{\mathrm{P}}^0\\ \hat{b}_{\mathrm{P}}^0\\ \hat{a}_{\mathrm{S}}^1\\ \hat{b}_{\mathrm{S}}^1\end{bmatrix} = -\frac{i\omega}{\epsilon^2\overline{c_{\mathrm{S}}}}\begin{bmatrix}\mathbf{H}_{\mathrm{SS}}^0 & \mathbf{0_2} & \mathbf{0_2} & \mathbf{0_2}\\ \mathbf{H}_{\mathrm{PS}}^1 & \mathbf{H}_{\mathrm{PP}}^0 & \mathbf{0_2} & \mathbf{0_2}\\ \mathbf{0_2} & \mathbf{0_2} & \mathbf{H}_{\mathrm{PP}}^0 & \mathbf{0_2}\\ \mathbf{0_2} & \mathbf{0_2} & \mathbf{H}_{\mathrm{SP}}^1 & \mathbf{H}_{\mathrm{SS}}^0\end{bmatrix}\begin{bmatrix}\hat{a}_{\mathrm{S}}^0\\ \hat{b}_{\mathrm{S}}^0\\ \hat{a}_{\mathrm{P}}^1\\ \hat{b}_{\mathrm{P}}^1\\ \hat{a}_{\mathrm{P}}^0\\ \hat{b}_{\mathrm{P}}^0\\ \hat{a}_{\mathrm{S}}^1\\ \hat{b}_{\mathrm{S}}^1\end{bmatrix} \tag{B.6}$$

where:

$$\mathbf{H}^0_{\mathrm{SS}} = \begin{bmatrix} \Delta^{(+)}_{\mu} - 1 & \Delta^{(-)}_{\mu} e^{-2i\omega z/\overline{c_{\mathrm{S}}}} \\ -\Delta^{(-)}_{\mu} e^{2i\omega z/\overline{c_{\mathrm{S}}}} & 1 - \Delta^{(+)}_{\mu} \end{bmatrix} \tag{B.7}$$

$$\mathbf{H}^0_{\mathrm{PP}} = \begin{bmatrix} \overline{\alpha}(\Delta^{(+)}_{K} - 1) & \overline{\alpha}\Delta^{(-)}_{K} e^{-2i\omega z/\overline{c_{\mathrm{P}}}} \\ -\overline{\alpha}\Delta^{(-)}_{K} e^{-2i\omega z/\overline{c_{\mathrm{P}}}} & \overline{\alpha}(1 - \Delta^{(+)}_{K}) \end{bmatrix} \tag{B.8}$$

$$\mathbf{H}^1_{\mathrm{SP}} = \begin{bmatrix} \Delta^{(+)} e^{i\omega z/\delta^-_c} & -\Delta^{(-)} e^{i\omega z/\delta^+_c} \\ -\Delta^{(-)} e^{-i\omega z/\delta^+_c} & \Delta^{(+)} e^{-i\omega z/\delta^-_c} \end{bmatrix} \tag{B.9}$$

$$\mathbf{H}^1_{\mathrm{PS}} = \begin{bmatrix} \Delta^{(+)} e^{-i\omega z/\delta^-_c \epsilon^2} & \Delta^{(-)} e^{i\omega z/\delta^+_c} \\ \Delta^{(-)} e^{-i\omega z/\delta^+_c \epsilon^2} & \Delta^{(+)} e^{i\omega z/\delta^-_c} \end{bmatrix} \tag{B.10}$$

and

$$\Delta^{(\pm)}_{\mu}(z) = \frac{1}{2}\left(1 \pm (1 + \epsilon\nu(z))\right), \quad \Delta^{(\pm)}_{K}(z) = \frac{1}{2}\left(1 \pm (1 + \epsilon\nu_K(z))\right) \tag{B.11}$$

and

$$\sqrt{\overline{\alpha}}\Delta^{(\pm)} = \pm\overline{\alpha}^2\epsilon\left(\nu_K(z) - \nu(z)\right) - \overline{\alpha}\left(-\epsilon\nu(z) \pm \epsilon\overline{\alpha}\nu_K(z)\right) \tag{B.12}$$

Considering the first block of the matrix Eq. B.6 corresponding to the Eq. 44 including heterogeneous P-wave modulus, the propagator $\mathbf{P}^{\epsilon}_{\mathrm{SV}}(z)$ is given by :

$$\mathbf{P}^{\epsilon}_{\mathrm{SV}}(z) = \begin{bmatrix} \alpha^{0,\epsilon}_{\mathrm{SV}}(z) & (\beta^{0,\epsilon}_{\mathrm{SV}}(z))^* & 0 & 0 \\ \beta^{0,\epsilon}_{\mathrm{SV}}(z) & (\alpha^{0,\epsilon}_{\mathrm{SV}}(z))^* & 0 & 0 \\ \alpha^{1,\epsilon}_{\mathrm{P}}(z) & -(\beta^{1,\epsilon}_{\mathrm{P}}(z))^* & \alpha^{0,\epsilon}_{\mathrm{P}}(z) & (\beta^{0,\epsilon}_{\mathrm{P}}(z))^* \\ \beta^{1,\epsilon}_{\mathrm{P}}(z) & -(\alpha^{1,\epsilon}_{\mathrm{P}}(z))^* & \beta^{0,\epsilon}_{\mathrm{P}}(z) & (\alpha^{0,\epsilon}_{\mathrm{P}}(z))^* \end{bmatrix}. \tag{B.13}$$

The definition of the propagator means that $\mathbf{P}^{\epsilon}_{\mathrm{SV}}(z)$ verifies the equation :

$$
\begin{aligned}
\frac{\mathrm{d}}{\mathrm{d}z}\mathbf{P}^{\epsilon}_{\mathrm{SV}}(z) &= \frac{\omega}{2\epsilon\overline{c_{\mathrm{S}}}}\nu(z)\left[\mathbf{h_0}^{\dagger} + \sin\left(\frac{2\omega z}{\epsilon^2\overline{c_{\mathrm{S}}}}\right)\mathbf{h_1}^{\dagger} + \cos\left(\frac{2\omega z}{\epsilon^2\overline{c_{\mathrm{S}}}}\right)\mathbf{h_2}^{\dagger}\right]\mathbf{P}^{\epsilon}_{\mathrm{SV}}(z) \\
&+ \frac{\omega}{2\epsilon\overline{c_{\mathrm{P}}}}\nu_K(z)\left[\mathbf{h_0} + \sin\left(\frac{2\omega z}{\epsilon^2\overline{c_{\mathrm{P}}}}\right)\mathbf{h_1} + \cos\left(\frac{2\omega z}{\epsilon^2\overline{c_{\mathrm{P}}}}\right)\mathbf{h_2}\right]\mathbf{P}^{\epsilon}_{\mathrm{SV}}(z) \\
&+ \frac{\omega}{\epsilon\overline{c_{\mathrm{S}}}}\nu(z)\left[\left(-\overline{\alpha}^{1/2} - \overline{\alpha}^{3/2}\right)\sin\left(\frac{\omega z}{\epsilon^2\delta_c^+}\right)\mathbf{h_3} + \left(-\overline{\alpha}^{1/2} - \overline{\alpha}^{3/2}\right)\cos\left(\frac{\omega z}{\epsilon^2\delta_c^+}\right)\mathbf{h_4}\right. \\
&\left.+ \left(-\overline{\alpha}^{1/2} + \overline{\alpha}^{3/2}\right)\sin\left(\frac{\omega z}{\epsilon^2\delta_c^-}\right)\mathbf{h_5} + \left(-\overline{\alpha}^{1/2} + \overline{\alpha}^{3/2}\right)\cos\left(\frac{\omega z}{\epsilon^2\delta_c^-}\right)\mathbf{h_6}\right]\mathbf{P}^{\epsilon}_{\mathrm{SV}}(z) \\
&+ \frac{\omega}{\epsilon\overline{c_{\mathrm{S}}}}\nu_K(z)\left[\left(-\overline{\alpha}^{1/2} + \overline{\alpha}^{3/2}\right)\sin\left(\frac{\omega z}{\epsilon^2\delta_c^+}\right)\mathbf{h_3} + \left(-\overline{\alpha}^{1/2} + \overline{\alpha}^{3/2}\right)\cos\left(\frac{\omega z}{\epsilon^2\delta_c^+}\right)\mathbf{h_4}\right. \\
&\left.+ \left(\overline{\alpha}^{1/2} - \overline{\alpha}^{3/2}\right)\sin\left(\frac{\omega z}{\epsilon^2\delta_c^-}\right)\mathbf{h_5} + \left(\overline{\alpha}^{1/2} - \overline{\alpha}^{3/2}\right)\cos\left(\frac{\omega z}{\epsilon^2\delta_c^-}\right)\mathbf{h_6}\right]\mathbf{P}^{\epsilon}_{\mathrm{SV}}(z)
\end{aligned}
\tag{B.14}
$$

Where $\mathbf{h}_i$ are the same than Eq. (52). Following the work the limit of small ϵ, the solution $\mathbf{P}^{\epsilon}_{\mathrm{SV}}(z)$ converges to the solution $\mathbf{P}_{\mathrm{SV}}(z)$ of the following stochastic differential equation:

$$
\begin{aligned}
\mathrm{d}\mathbf{P}_{\mathrm{SV}}(0,z) &= \frac{\omega\sqrt{\gamma(0)}}{2\overline{c_{\mathrm{S}}}}\mathbf{h}_0^{\dagger}\mathbf{P}_{\mathrm{SV}}\circ\mathrm{d}W_0(z) + \frac{\omega\sqrt{\gamma(\omega)}}{2\sqrt{2}\overline{c_{\mathrm{S}}}}\mathbf{h}_1^{\dagger}\mathbf{P}_{\mathrm{SV}}\circ\mathrm{d}W_1(z) + \frac{\omega\sqrt{\gamma(\omega)}}{2\sqrt{2}\overline{c_{\mathrm{S}}}}\mathbf{h}_2^{\dagger}\mathbf{P}_{\mathrm{SV}}\circ\mathrm{d}\tilde{W}_1(z) \\
&+ \frac{\omega\sqrt{\gamma_K(0)}}{2\overline{c_{\mathrm{P}}}}\mathbf{h}_0\mathbf{P}_{\mathrm{SV}}\circ\mathrm{d}W_2(z) + \frac{\omega\sqrt{\gamma_K(\omega)}}{2\sqrt{2}\overline{c_{\mathrm{P}}}}\mathbf{h}_1\mathbf{P}_{\mathrm{SV}}\circ\mathrm{d}W_3(z) + \frac{\omega\sqrt{\gamma_K(\omega)}}{2\sqrt{2}\overline{c_{\mathrm{P}}}}\mathbf{h}_2\mathbf{P}_{\mathrm{SV}}\circ\mathrm{d}\tilde{W}_3(z) \\
&+ \frac{\omega}{\sqrt{2}\overline{c_{\mathrm{S}}}}\sqrt{\left(\overline{\alpha}^{1/2} + \overline{\alpha}^{3/2}\right)^2\gamma_+(\omega) + \left(-\overline{\alpha}^{1/2} + \overline{\alpha}^{3/2}\right)^2\gamma_{K+}(\omega)}\mathbf{h}_3\mathbf{P}_{\mathrm{SV}}\circ\mathrm{d}W_6(z) \\
&+ \frac{\omega}{\sqrt{2}\overline{c_{\mathrm{S}}}}\sqrt{\left(\overline{\alpha}^{1/2} + \overline{\alpha}^{3/2}\right)^2\gamma_+(\omega) + \left(-\overline{\alpha}^{1/2} + \overline{\alpha}^{3/2}\right)^2\gamma_{K+}(\omega)}\mathbf{h}_4\mathbf{P}_{\mathrm{SV}}\circ\mathrm{d}\tilde{W}_6(z) \\
&+ \frac{\omega}{\sqrt{2}\overline{c_{\mathrm{S}}}}\sqrt{\left(-\overline{\alpha}^{1/2} + \overline{\alpha}^{3/2}\right)^2\gamma_+(\omega) + \left(\overline{\alpha}^{1/2} - \overline{\alpha}^{3/2}\right)^2\gamma_{K+}(\omega)}\mathbf{h}_5\mathbf{P}_{\mathrm{SV}}\circ\mathrm{d}W_7(z) \\
&+ \frac{\omega}{\sqrt{2}\overline{c_{\mathrm{S}}}}\sqrt{\left(-\overline{\alpha}^{1/2} + \overline{\alpha}^{3/2}\right)^2\gamma_+(\omega) + \left(\overline{\alpha}^{1/2} - \overline{\alpha}^{3/2}\right)^2\gamma_{K+}(\omega)}\mathbf{h}_6\mathbf{P}_{\mathrm{SV}}\circ\mathrm{d}\tilde{W}_7(z) \\
&- \frac{\gamma^{(s)}\omega^2}{8\overline{c_{\mathrm{S}}}^2}\mathbf{h}_0^{\dagger}\mathbf{P}_{\mathrm{SV}}\mathrm{d}z - \frac{\gamma_K^{(s)}\omega^2}{8\overline{c_{\mathrm{P}}}^2}\mathbf{h}_0\mathbf{P}_{\mathrm{SV}}\mathrm{d}z \\
&- i\frac{\omega^2}{2\overline{c_{\mathrm{S}}}^2}\left[\left(\overline{\alpha}^{1/2} + \overline{\alpha}^{3/2}\right)^2\gamma_+^{(s)}(\omega) + \left(-\overline{\alpha}^{1/2} + \overline{\alpha}^{3/2}\right)^2\gamma_{K+}^{(s)}(\omega)\right]\mathbf{h}_5\mathbf{P}_{\mathrm{SV}}\mathrm{d}z
\end{aligned}
\tag{B.15}
$$

Where $\gamma(\omega), \gamma^{(s)}(\omega), \gamma_{\pm}(\omega)$ are defined Eq. (55) and :

$$\begin{aligned}
\gamma_K(\omega) &= 2\int_0^{+\infty} C_{\nu_K} \cos\left(\frac{2\omega z}{\overline{c_{\mathrm{P}}}}\right) \mathrm{d}z, \quad \gamma_K^{(s)}(\omega) = 2\int_0^{+\infty} C_{\nu_K} \sin\left(\frac{2\omega z}{\overline{c_{\mathrm{P}}}}\right) \mathrm{d}z \\
\gamma_{K\pm}(\omega) &= 2\int_0^{+\infty} C_{\nu_K} \cos\left(\frac{\omega z}{\delta_c^{\pm}}\right) \mathrm{d}z, \quad \gamma_{K\pm}^{(s)}(\omega) = 2\int_0^{+\infty} C_{\nu_K} \sin\left(\frac{\omega z}{\delta_c^{\pm}}\right) \mathrm{d}z
\end{aligned} \tag{B.16}$$